

# Visualized Image Processing for images from Backward Facing Step Combuster

November 25, 2017

## Contents

<b>1</b>	<b>Aim</b>	<b>2</b>
<b>2</b>	<b>Experimental Setup</b>	<b>2</b>
2.1	Backward Facing Step Combustor . . . . .	2
2.1.1	Settling Chamber . . . . .	3
2.1.2	Inlet Section . . . . .	3
2.1.3	Inlet Optical Access Module (IOAM) . . . . .	3
2.1.4	Test Section . . . . .	4
2.1.5	Air and Fuel Supply . . . . .	4
2.1.6	Acetone seeder . . . . .	5
2.2	Optical Setup . . . . .	5
2.2.1	Unsteady Pressure Measurements . . . . .	5
2.2.2	Simultaneous time-resolved particle image velocimetry (TR-PIV) and CH* chemiluminescence imaging . . . . .	6
2.2.3	Time-resolved particle image velocimetry (TR-PIV) . . . . .	6
2.2.4	Time-resolved CH* chemiluminescence imaging . . . . .	7
<b>3</b>	<b>Theory</b>	<b>7</b>
3.1	Cross-correlation . . . . .	7
3.2	Image preprocessing techniques . . . . .	8
3.2.1	Image quality parameters . . . . .	8
<b>4</b>	<b>Analysis:</b>	<b>8</b>
4.1	Raw Images . . . . .	9
4.2	Outlier Removal . . . . .	13
4.3	Image Enhancement . . . . .	16

4.3.1	Intensity Histogram equalization . . . . .	17
4.3.2	Sharpening . . . . .	22
4.4	Image Filtering . . . . .	26
4.4.1	Order statistics filters . . . . .	26
4.4.2	Low and High Pass filters . . . . .	41
<b>5</b>	<b>Results</b>	<b>51</b>
<b>6</b>	<b>Conclusion</b>	<b>53</b>
<b>7</b>	<b>Analysis Code</b>	<b>53</b>

## 1 Aim

To analyse the raw images from an experiment in backward facing step combustor under with premixed flame instabilities and vortex shedding taking place and plot the velocity field at a particular instant using basic image processing techniques.

## 2 Experimental Setup

### 2.1 Backward Facing Step Combustor

In this experiment a backward facing step combustor is used with non-reacting flow. The combustor configuration is as follows,

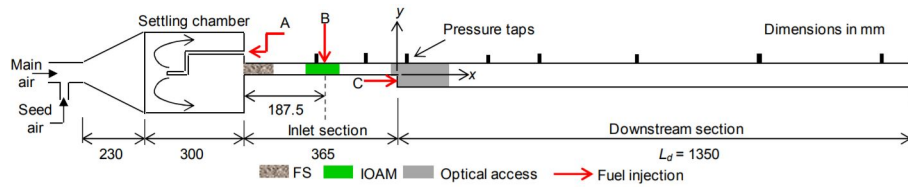


Figure 1: Combustor configuration

The combustor length  $L_d = 1350\text{mm}$

The length of the inlet section  $l_i = 365\text{mm}$

The settling chamber(tank) length  $l_t = 530\text{mm}$

The combustor employs flow straighteners at the tank exit and we have two optically accessible fields, one at the inlet and the other at the shear layer near the combustor opening. The field of view is located in the later. The dimensions of the field of view are  $l_f = 120\text{mm} \times h_f = 60\text{mm}$ .

### 2.1.1 Settling Chamber

The settling chamber consists of a cone-cylinder arrangement. The conical section acts as a diffuser with an inlet diameter  $d_{t,i} = 25.4\text{mm}$  that expands to  $d_{t,e} = 200\text{mm}$  diameter over a length of  $l_{t,cone} = 230\text{mm}$ . This includes a half cone angle of  $\theta_{t,cone} = 20^\circ$ , which causes a smooth expansion of the flow. The cylindrical section attached to the cone spans  $l_{t,cyl} = 300\text{mm}$  in length, leading to the inlet section of the combustor. The inlet section of cross sectional area  $l_{c,i} = 30\text{mm} \times h_{c,i} = 60\text{mm}$  is mounted at the exit of the cylindrical portion. The area ratio between the cylindrical portion and the inlet section is  $\frac{A_{t,e}}{A_{c,i}} = 17.45$ .

### 2.1.2 Inlet Section

The inlet section has a cross sectional area  $l_{c,i} = 30\text{mm} \times h_{c,i} = 60\text{mm}$ , The length of the inlet section is  $l_i = 400\text{mm}$ . It carries flow straighteners.

**Flow Straighteners** They primarily consist of a honeycomb shaped mesh with some other meshes that quieten the flow perturbations at high possible upstream point i.e the tank exit. The honeycomb is tight-fitted to the inlet section, while the meshes are mounted on frames that are inserted into grooves cut on the walls of the inlet duct. The top plate of the section is held by a set of allen screws, so that it can be opened to remove the meshes for cleaning or replacement. The honeycomb has a cell size of  $c_d = 4\text{mm}$  diameter and a length of  $c_l = 25\text{mm}(\approx 8d)$  to reduce lateral turbulence components of the flow and also to straighten the flow. At a distance of  $20\text{mm}$  from the honeycomb, three consecutive meshes are arranged at a distance of  $35\text{mm}$  each. These are progressively finer along the flow direction: the mesh sizes are  $600, 200, 140\mu\text{m}$ , with an open area ratio of  $60 - 65\%$ . They reduce the perturbation in the longitudinal turbulence component to a greater extent than the lateral component but result in a slight pressure drop. The pressure drop of the flow through the honeycomb is relatively lower as compared to that through a mesh. The pressure drop coefficient for a mesh for the velocity range  $0 < U < 20\text{m/s}$  can be expressed as (Mehta,1985)

$$K = 6.5 \left( \frac{1 - \beta}{\beta^2} \right) \left( \frac{U d_m}{\beta \nu} \right)^{-\frac{1}{3}} \quad (1)$$

where,

$\beta$  = open area ratio (which must be  $> 0.58$  to avoid rippling effect)

$d_m$  = diameter of mesh opening

$\nu$  = kinematic viscosity

$U$  = velocity of airflow

These meshes reduce the turbulence level to  $\sim 10\%$ .

### 2.1.3 Inlet Optical Access Module (IOAM)

The IOAM is  $100\text{mm}$  long and has the same cross sectional dimensions as the inlet duct( $l_{c,i} = 30\text{mm} \times h_{c,i} = 60\text{mm}$ ). It has provision for optical access that uses quartz windows fitted to the sides walls and slits at

the top and bottom walls that carry quartz strips for the laser light sheet to pass through. The IOAM is used for the measuring the turbulence level of the inlet flow downstream of the meshes. A pressure port is provided on a stainless steel side plate at 25mm distance from the inlet of the IOAM.

#### 2.1.4 Test Section

The test section is 370mm long. A step 30mm high and 60mm wide is attached to the bottom wall that covers a distance of 40mm from its inlet. The combustor cross-section downstream of the step is  $l_{c,e} = 60\text{mm} \times h_{c,e} = 60\text{mm}$ . The test section has an optical access of size 350mm  $\times$  4mm at the mid portion of the top and bottom walls of the test section for the laser light sheet to pass through. In addition, the side walls have glass windows of size  $l_f = 150\text{mm} \times h_f = 60\text{mm}$  for imaging purposes, indicated by the grey shaded region in Figure (1).

#### 2.1.5 Air and Fuel Supply

A two-stage reciprocating compressor supplies compressed air at 12bar storage pressure after dehumidification. A gate valve of 4" diameter is used between the outlet of the reservoir and the inlet to the combustor. A combination of air filters are used, followed by a dehumidifier upstream to the combustor inlet.

The reactants, namely, air and methane, are issued into the combustor using mass flow controllers (MFC) for the full operating range of 0–4000lpm (litres per minute) for air and 0–100lpm for methane. For the laser diagnostics involving time-resolved particle image velocimetry (TRPIV), an additional MFC in the operating range of 0 – 100lpm is used for carrying the seeded flow. The main air stream supply is adjusted for the seeding air flow rate accordingly. For the acetone planar laser induced fluorescence (PLIF) experiments, methane flows through the acetone bath before it is supplied into the combustor.

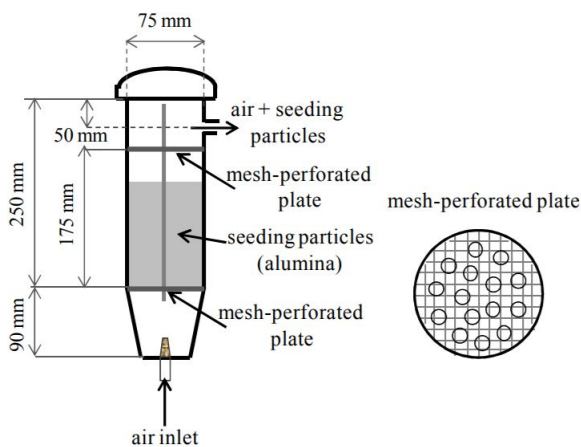


Figure 2: Fluidized Bed Seeder

**Fluidized bed seeder** A fluidized bed seeder is used to introduce the seeding particles into the flow for the velocity measurements using the PIV technique. For the seeding, 1 – 2 $\mu\text{m}$  sized alumina particles are used and an additional air supply line is provided to the seeder. The fluidized bed seeder shown in Figure(2).

### 2.1.6 Acetone seeder

Figure (3) shows the acetone seeder. Fuel is issued into a liquid acetone bath through a series of eight holes of  $1.5\text{mm}$  diameter each. The fuel forms bubbles through the acetone that bursts as it rises in the bath. Subsequently, the acetone vaporizes and mixes with the fuel, and this mixture is injected at locations *A*, *B* and *C* for performing the planar laser induced fluorescence experiments.

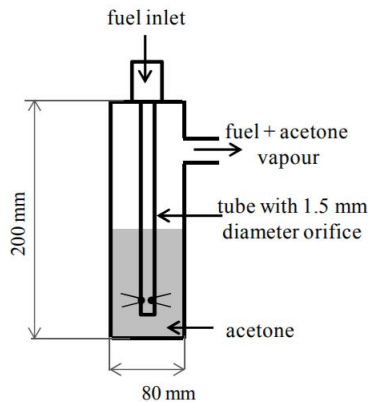


Figure 3: Acetone Seeder

## 2.2 Optical Setup

### 2.2.1 Unsteady Pressure Measurements

The pressure measurements are obtained using the piezo-electric transducer (103B02 model, PCB make,  $225\text{mV}/\text{kPa}$  sensitivity). The pressure-time traces acquired as analog signals are conditioned by the signal conditioner. The output of the signal conditioner is routed to the data acquisition system that has a National instruments (NI) analog-to-digital (A/D) converter card fitted in a PCI slot of a computer. The card performs the A/D conversion at  $12\text{bit}$  resolution in the  $\pm 5\text{V}$  range with a conversion speed of  $10\mu\text{s}/\text{channel}$ .

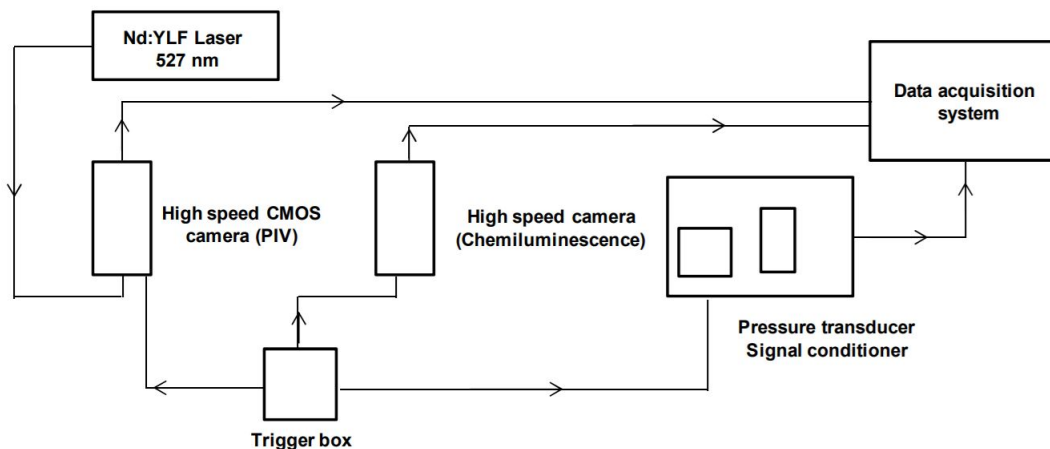


Figure 4: Schematic of simultaneous imaging using TR-PIV and  $\text{CH}^*$  chemiluminescence

## 2.2.2 Simultaneous time-resolved particle image velocimetry (TR-PIV) and CH\* chemiluminescence imaging

The schematic shown in Figure(4) comprises the simultaneous TR-PIV and CH\* chemiluminescence imaging along with the unsteady pressure measurements. The TR-PIV 58 measurement system consists of a high-speed laser synchronized with high-speed camera through frame straddling. For the CH\* chemiluminescence imaging, additional high-speed camera is used. Both the high-speed cameras are connected to separate data acquisition system, which in addition, also includes the pressure measurements. The cameras and the pressure measurement system are triggered using a trigger box.

The timing diagram for the TR-PIV and the chemiluminescence imaging is shown in Figure(5). For the TR-PIV experiments, the delay settings on the laser system are adjusted such that the first laser pulse occurs near the falling edge and the second subsequent pulse falls near the rising edge of the camera exposure. This is known as frame straddling, and is typically used in TR-PIV. The exposure time of the camera is denoted by  $T_{exp}$  and the pulse delay between the successive laser pulses is  $T_{del}$ . A trigger pulse of 5V TTL is issued to the TR-PIV/CH\* chemiluminescence imaging along with the pressure measuring system to ensure that all the measurements are simultaneous in nature.

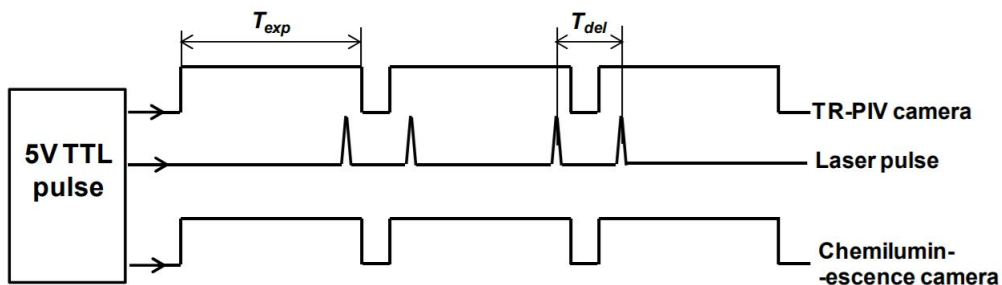


Figure 5: Timing Diagram

## 2.2.3 Time-resolved particle image velocimetry (TR-PIV)

For the laser diagnostics involving TR-PIV, the FOV is chosen to be  $l_{fv} = 120mm \times h_{fv} = 60mm$ , which is sufficient to capture the entire recirculation zone. For performing the TR-PIV, we use a single-cavity Nd:YLF laser of wavelength 527nm operated in the twin pulse mode at 3000pulse-pairs/s. We form the laser light sheet by a combination of spherical convex and concave lenses followed by a cylindrical lens, as shown in Figure(6). The light sheet thickness at its waist is  $\sim 1mm$  and is 250mm long.

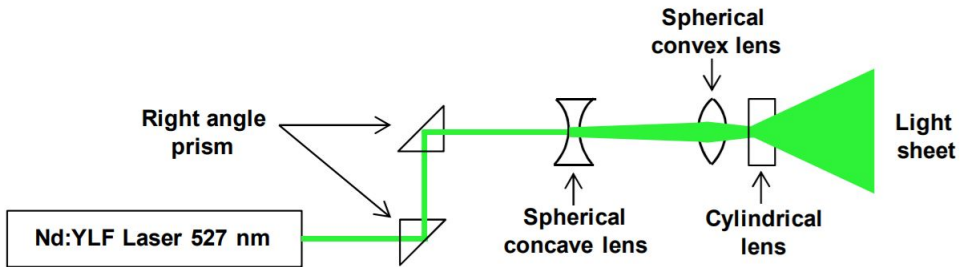


Figure 6: Schematic of laser optics for TR-PIV

We use a high-speed CMOS camera (Phantom V12.1) to acquire the Mie scattering intensity of the seeded particles operated at the full resolution of  $1280 \times 800$  pixels. Along with this camera, we use a Nikkor lens of  $50\text{mm}$  diameter and an aperture with the focal length to diameter ratio of 1.2. The synchronization of the laser and camera is done using frame straddling, which is achieved by using the clock pulse of the laser to trigger the camera.

#### 2.2.4 Time-resolved CH\* chemiluminescence imaging

To study the flame dynamics in the presence of an oscillating flow, a suitable technique is the digital chemiluminescence imaging to visualize the combustion process. For the oscillatory processes to uncover the physics of the phenomenon, high-speed digital chemiluminescence imaging is generally a stringent requirement. In the present study, for the heat release rate marker, the chemiluminescence of the CH\* flame radical is imaged. For this, we use a high-speed camera (Photron make) operated at a resolution of  $1024 \times 1024$  pixels and at a framing rate of  $3000$  frames/s. We use a Nikkor lens of  $50\text{mm}$  diameter with a maximum aperture with focal length to diameter ratio of 1.2. The time-resolved chemiluminescence is performed simultaneously with the TR-PIV and the unsteady pressure measurements. The data recording for each of these measurements is commenced at the same time using a 5V TTL pulse as a trigger signal.

## 3 Theory

### 3.1 Cross-correlation

Cross-correlation is a measure of similarity of two series as a function of the displacement of one relative to the other. This is also known as a sliding dot product or sliding inner-product. It is commonly used for searching a larger image for a shorter, known image. For continuous functions  $f$  and  $g$ , the cross-correlation is defined as,

$$(f \star g)(\tau) = \int_{-\infty}^{\infty} f^*(t)g(t + \tau)dt \quad (2)$$

, where  $f^*$  denotes the complex conjugate of  $f$ , and  $\tau$  is the displacement, also known as lag, although a positive value of  $\tau$  actually means that  $g(t + \tau)$  leads  $f(t)$ .

Similarly, for discrete functions, the cross-correlation is defined as,

$$(f * g)[n] = \sum_{m=-\infty}^{\infty} f^*[m]g[m+n] \quad (3)$$

### 3.2 Image preprocessing techniques

It is the use of computer algorithms to perform image processing on digital images. As a subcategory or field of digital signal processing, digital image processing has many advantages over analog image processing. It allows a much wider range of algorithms to be applied to the input data and can avoid problems such as the build-up of noise and signal distortion during processing. Since images are defined over two dimensions (perhaps more) digital image processing may be modeled in the form of multidimensional systems.

It involves but strictly not limited to,

- Image data conversion (RGB to Greyscale)
- Geometric transformations (Cropping)
- Image enhancement and filtering (Histogram Equalization, low pass filter)

#### 3.2.1 Image quality parameters

**Outlier percentage** Outlier percentage are basically ratio of the number of components that lie outside  $\pm n\sigma$  of the mean of the matrix values to the total number of components in the matrix.

## 4 Analysis:

We shall take the following two images from the data set given - Figure(7),(8)( arbitrarily). The images are taken on a  $120mm \times 60mm$  FOV at a time difference of  $\Delta t = 50\mu s$ . The resolution of both the images is  $1264 \times 592$ . From naked eye observation we see that edges are erroneous, there exists background intensity and the chemiluminiscence particle density seems to be lower below the step compared to the direct flow above it.



Figure 7: Image A

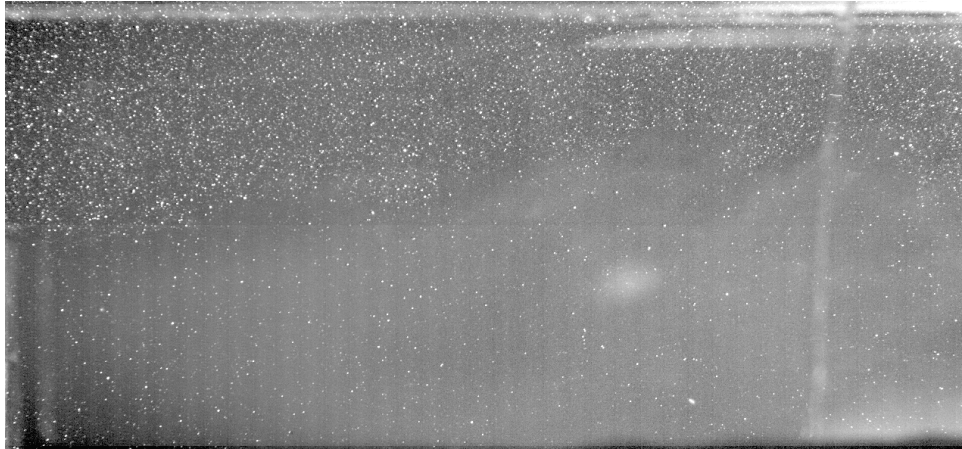


Figure 8: Image B

#### 4.1 Raw Images

Let us check the Intensity histogram of our raw images,

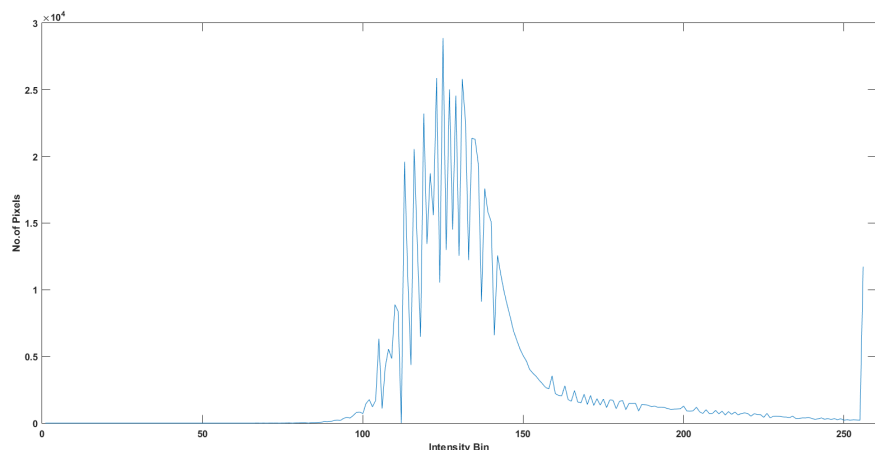


Figure 9: Intensity Histogram of A

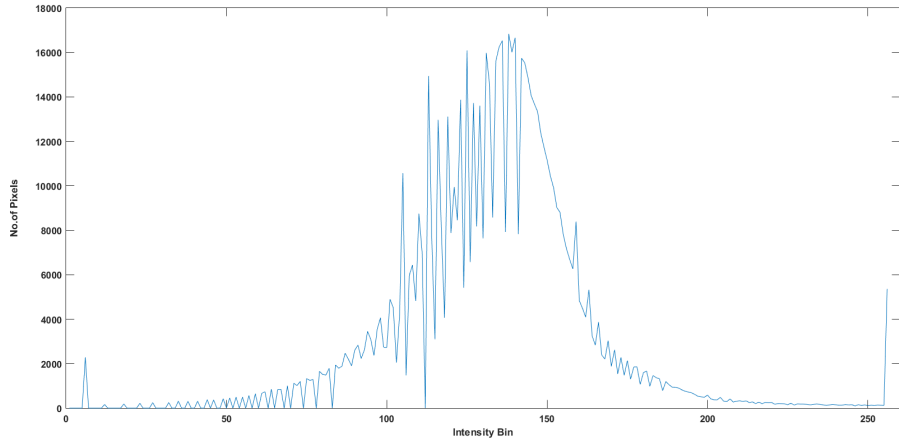


Figure 10: Intensity Histogram of B

We shall first check how our raw images perform in the cross correlation over grid sizes  $16 \times 16, 24 \times 24, 32 \times 32$ . We shall use qualitative parameters 'outlier %' and 'Standard deviation of the intensity histogram' for our results and basis for improvement. We take  $n = 0.95$  as it will the  $\pm 95\%$  of standard deviation outliers.

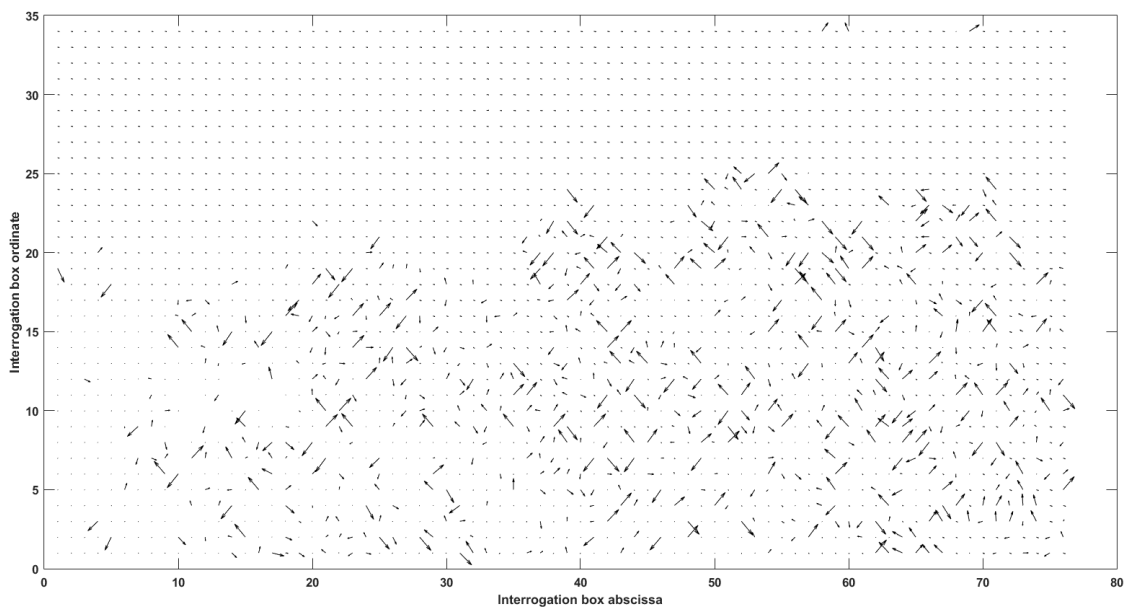


Figure 11: Vector field of raw image 16x16

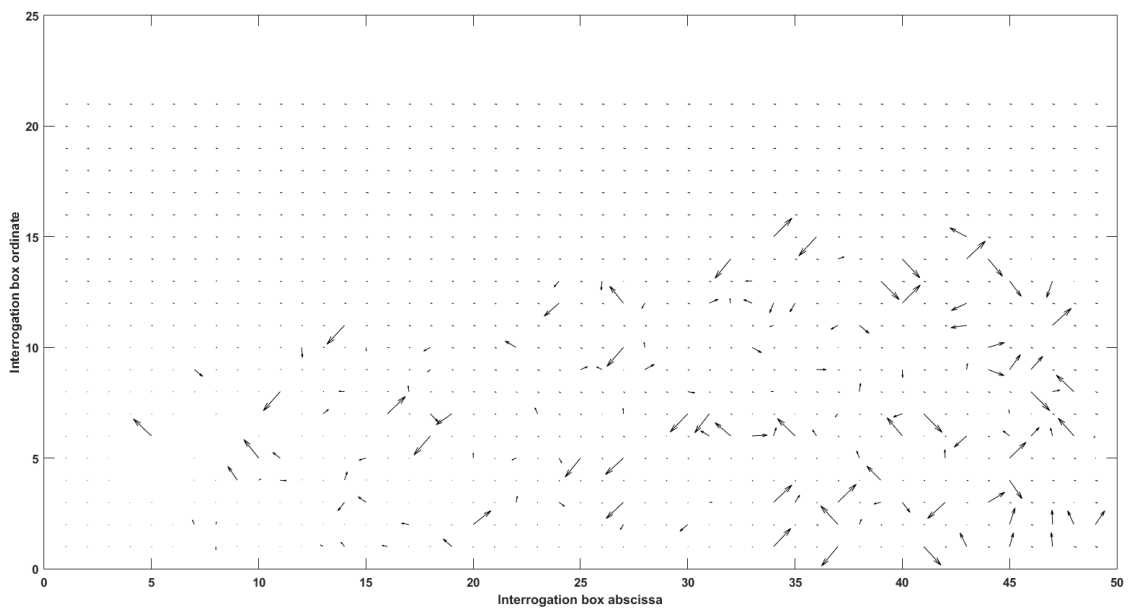


Figure 12: Vector field of raw image 24x24

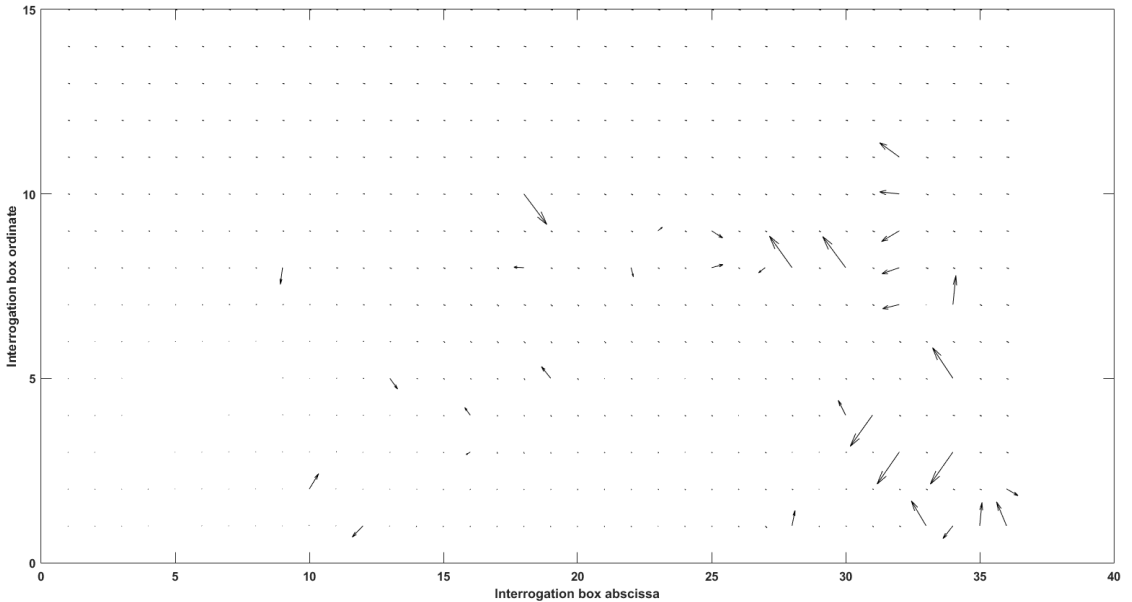


Figure 13: Vector field of raw image 32x32

Grid size	Outlier %	Histogram SD of image A	Histogram SD of image B
16x16	48.26	5.78E+03	4.50E+03
24x24	13.31	5.78E+03	4.50E+03
32x32	6.11	5.78E+03	4.50E+03

We now perform various image processing techniques to improve our outlier % (for valid measurements) and histogram standard deviations(for contrast).

## 4.2 Outlier Removal

We Now proceed to remove the outliers present in our images to  $\mu \pm \sigma$  where  $\mu$  is the mean displacement and  $\sigma$  the standard deviation of the displacement at each interrogation box. We have not modified the intensity values of our original images as of yet. We replace all outliers here with the mean in their corresponding axis.

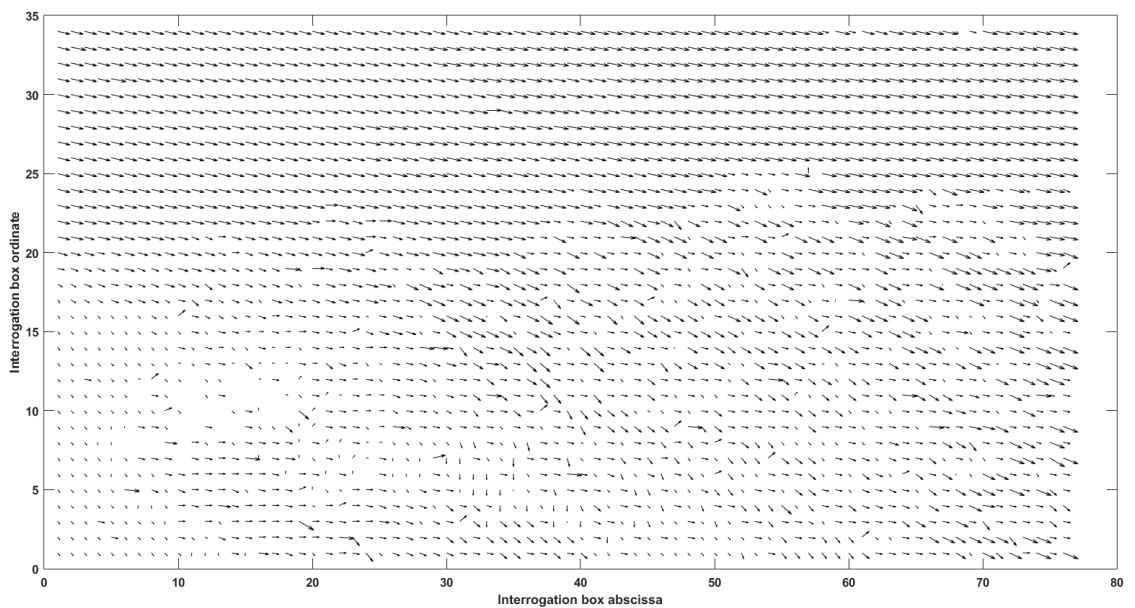


Figure 14: Vector field of interpolated image 16x16

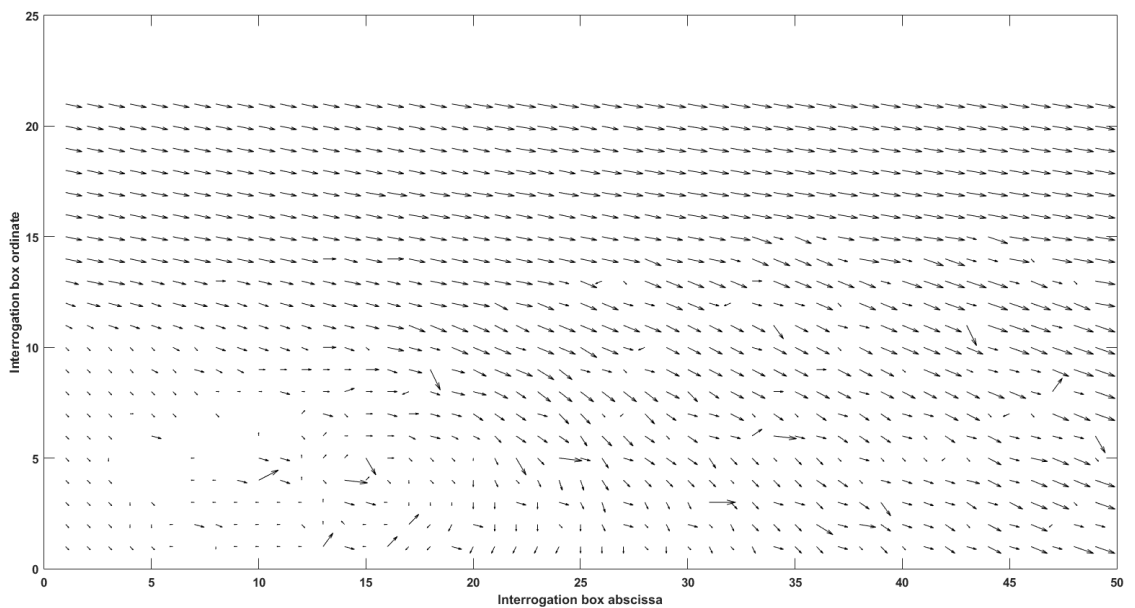


Figure 15: Vector field of interpolated image 24x24

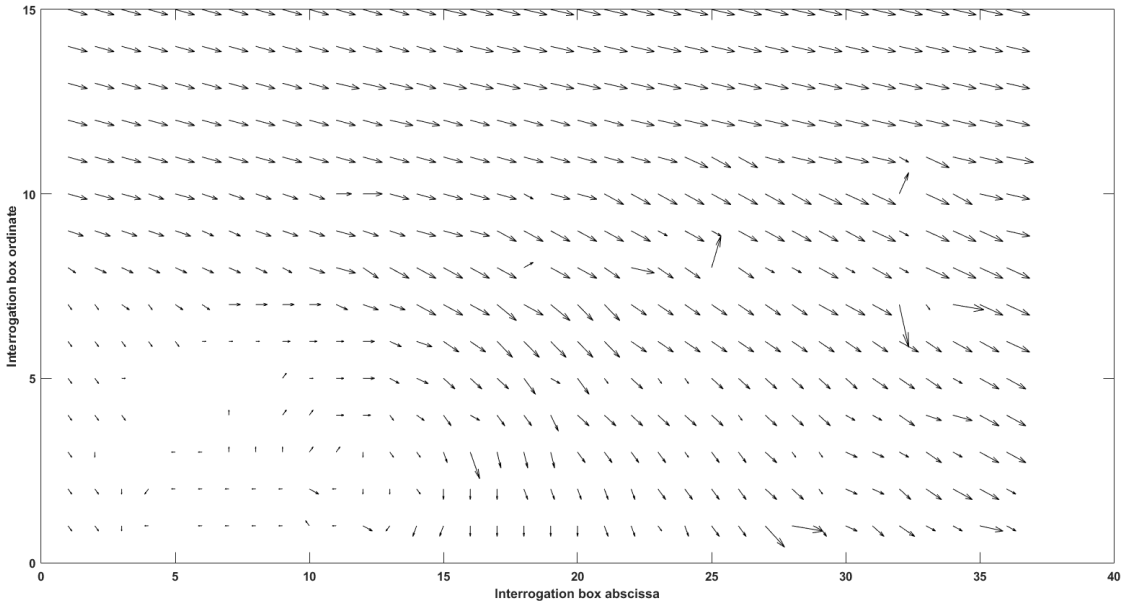


Figure 16: Vector field of interpolated image 32x32

Visually we can see great improvement in the vector fields and we shall statistically calculate and tabulate the new outlier vector percentages as follows,

Grid size	Outlier %	Histogram SD of image A	Histogram SD of image B
16x16	20.78	5.78E+03	4.50E+03
24x24	0.58	5.78E+03	4.50E+03
32x32	0.37	5.78E+03	4.50E+03

Which verifies that the quality of the vector fields has greatly improved. Having high outlier % at smaller grid sizes is inevitable because of the associated smaller matrices which can increase error in cross correlation. This can be reduced via overlapping of interrogation windows which we have not done in this analysis. From here on we shall use the  $24 \times 24$  grid for all further analysis.

### 4.3 Image Enhancement

Image enhancement techniques are used to improve an image, where “improve” can be defined objectively or subjectively. They can be implemented for various reasons from improving signal to noise ratio to implementations in edge detection. We use two widely used image enhancement methods namely histogram equalization and

image sharpening and we shall visually see how they affect/improve our current.

#### 4.3.1 Intensity Histogram equalization

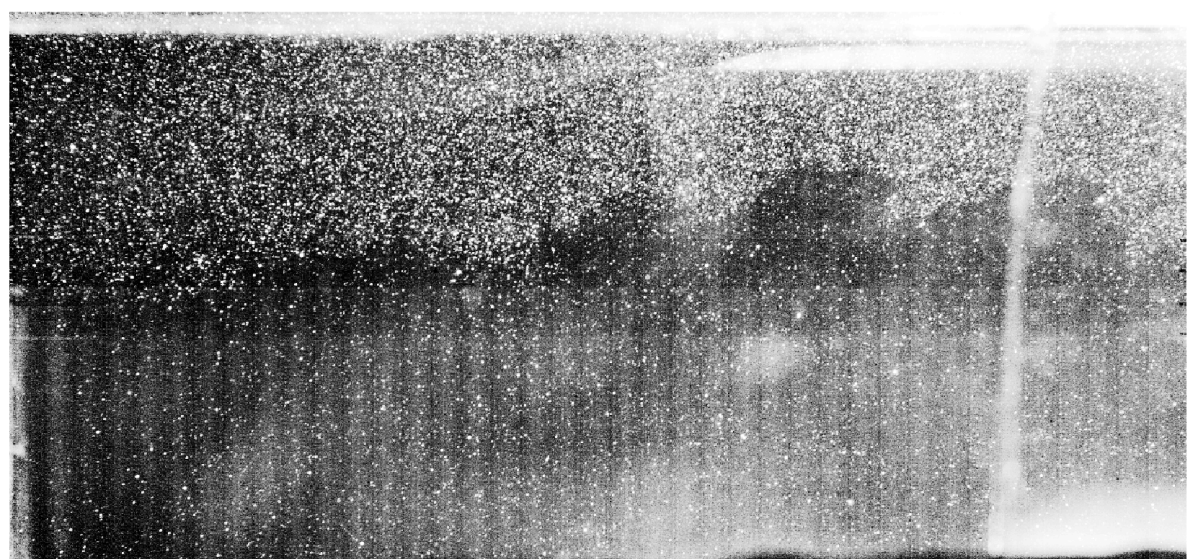


Figure 17: Histogram equalized image A

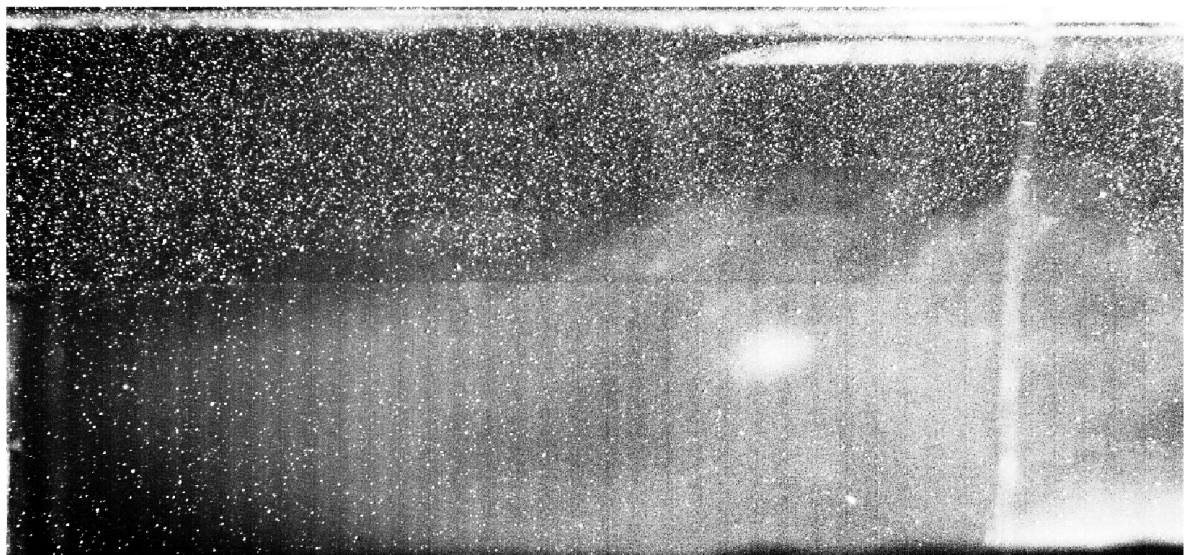


Figure 18: Histogram equalized image B

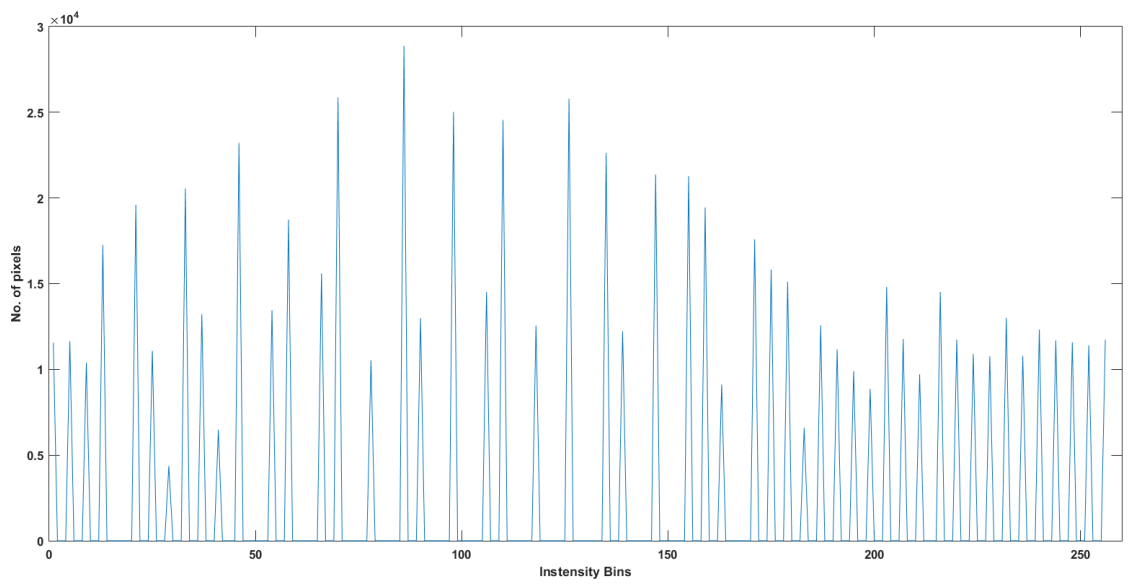


Figure 19: Intensity Histogram of A after histogram equalization

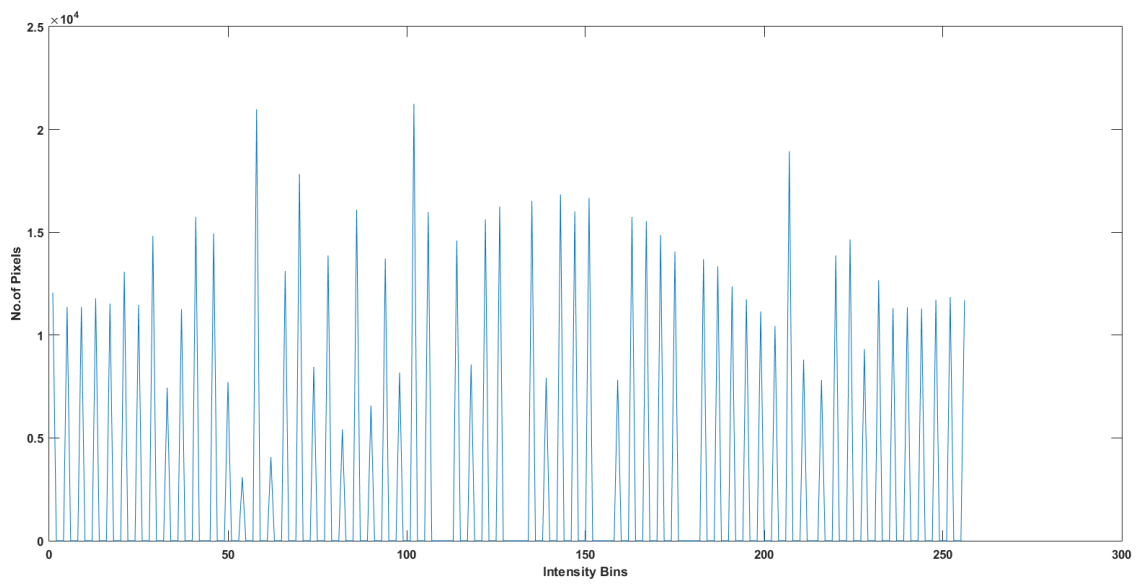


Figure 20: Intensity Histogram of B after histogram equalization

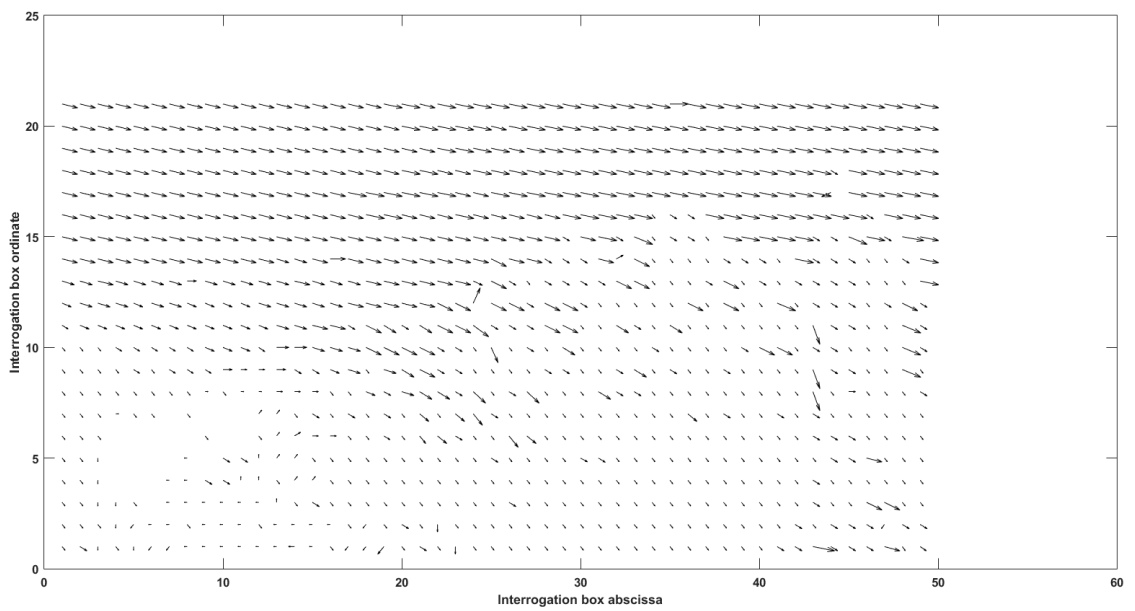


Figure 21: Vector field after histogram equalization

#### 4.3.2 Sharpening

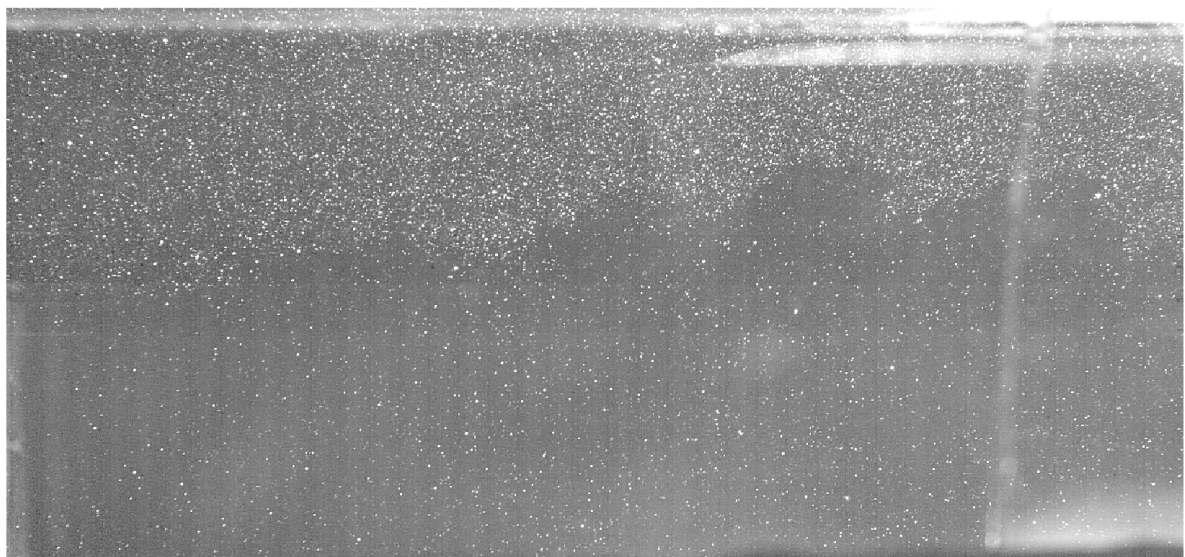


Figure 22: Sharpened image A

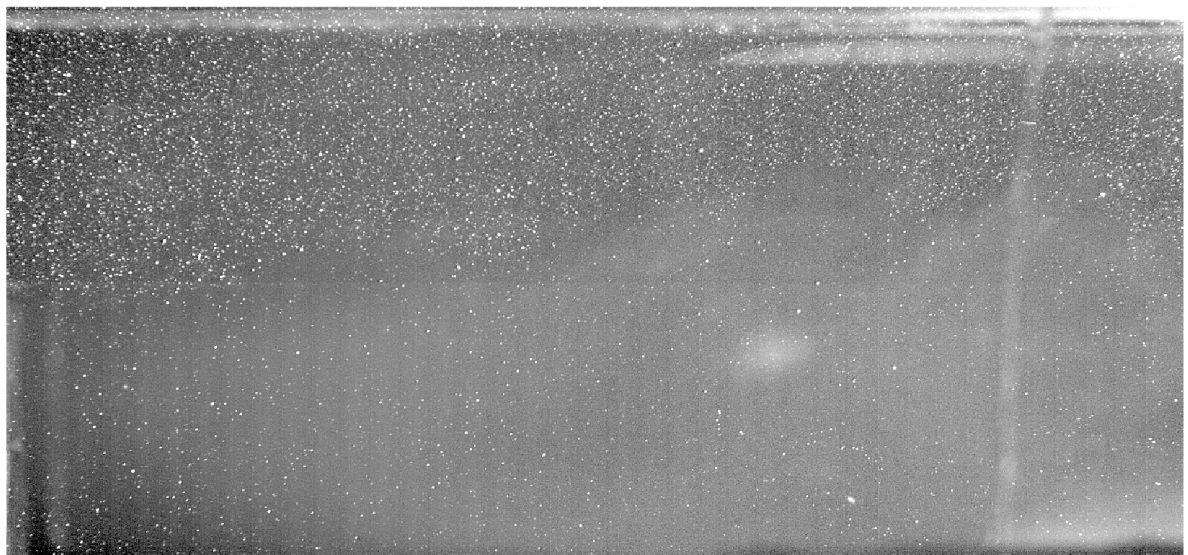


Figure 23: Sharpened image B

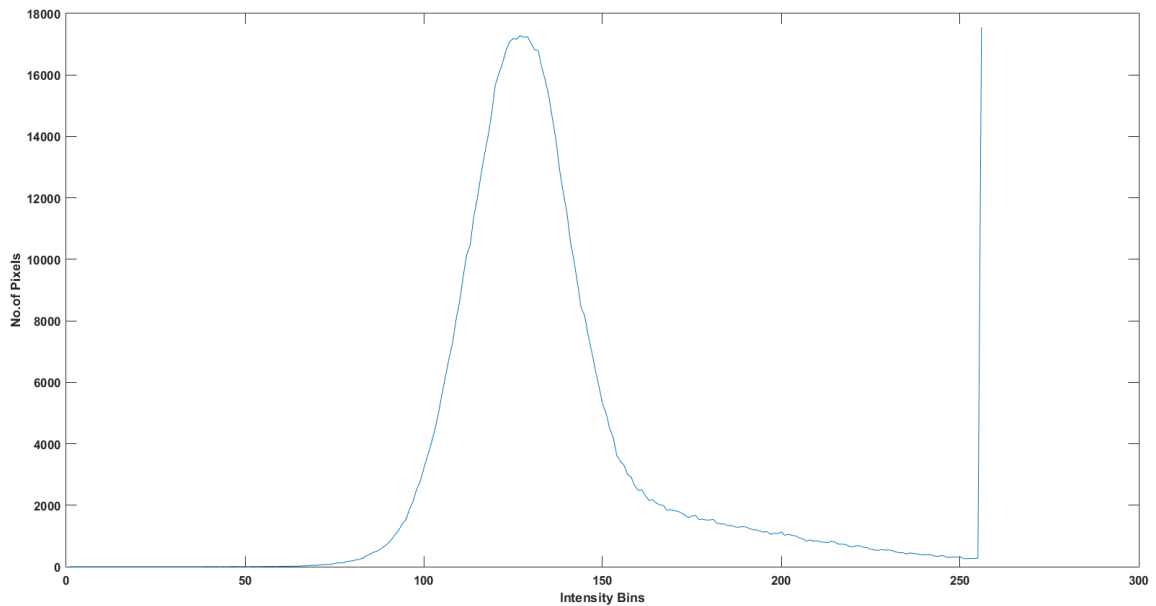


Figure 24: Intensity Histogram of A after sharpening

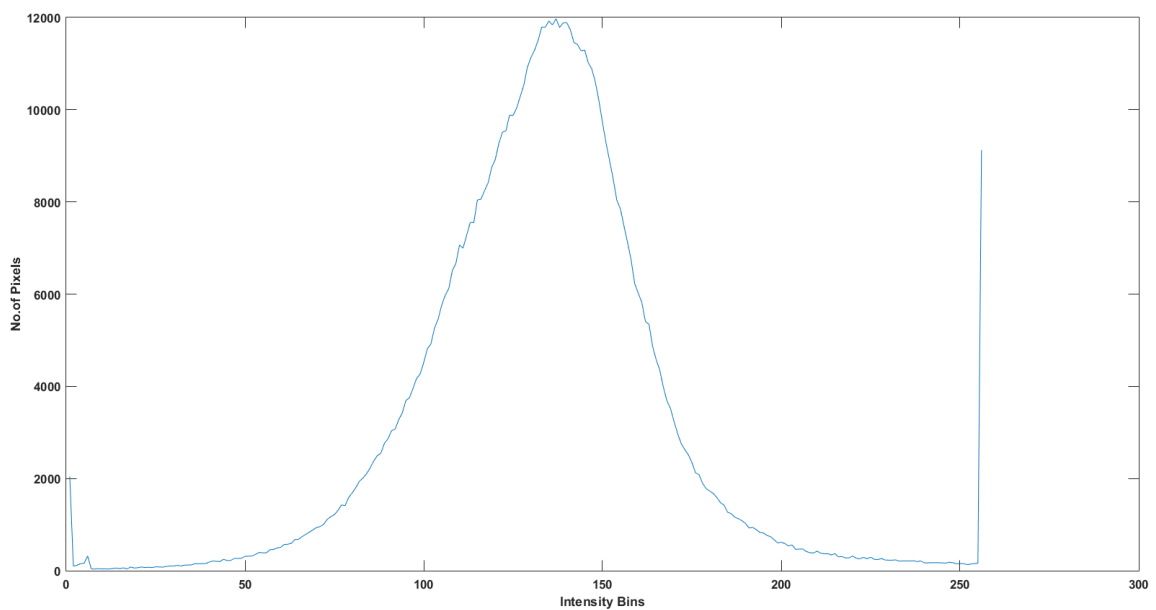


Figure 25: Intensity Histogram of B after sharpening

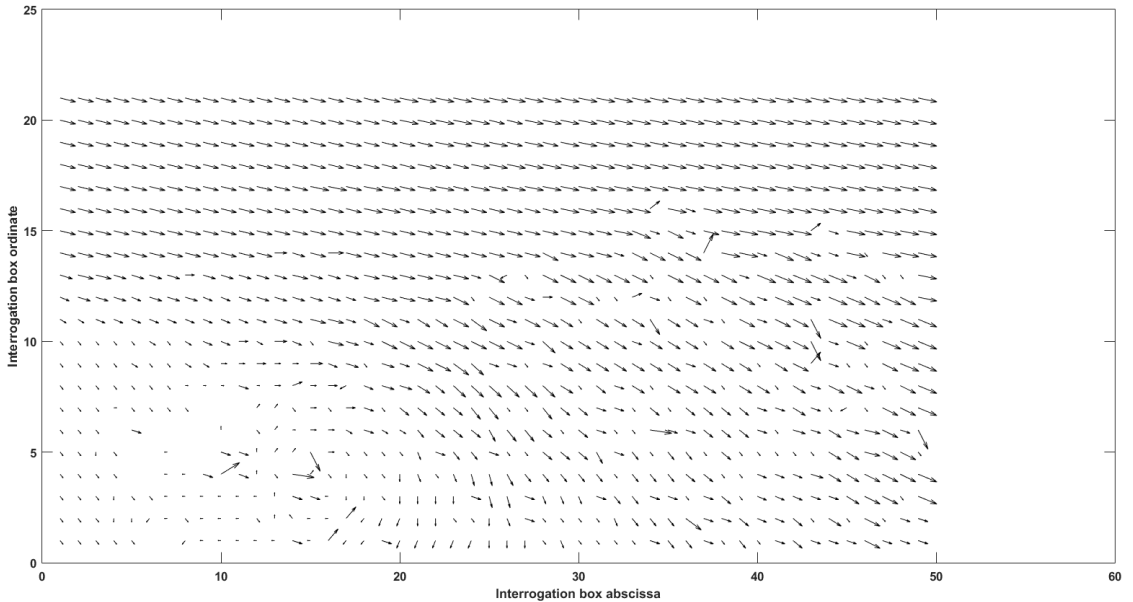


Figure 26: Vector field after Sharpening

Enhancement	Outlier %	Histogram SD of image A	Histogram SD of image B
Histogram Equalization	0.097	6.37E+03	5.60E+03
Sharpening	0	4.87E+03	3.76E+03

## 4.4 Image Filtering

Filtering is a technique for modifying or enhancing an image. For example, you can filter an image to emphasize certain features or remove other features. Image processing operations implemented with filtering include smoothing, sharpening, and edge enhancement. Filtering is a neighborhood operation, in which the value of any given pixel in the output image is determined by applying some algorithm to the values of the pixels in the neighborhood of the corresponding input pixel. A pixel's neighborhood is some set of pixels, defined by their locations relative to that pixel.

### 4.4.1 Order statistics filters

These are filters that have many different kinds of implementations but follow an order and select algorithm. On a  $3 \times 3$  box around the central pixel, the mean is the 5th order filter, the minimum is the 1st order filter and

the maximum being the 9th order filter upon a 1-9 ordering in the ascending order of intensities.

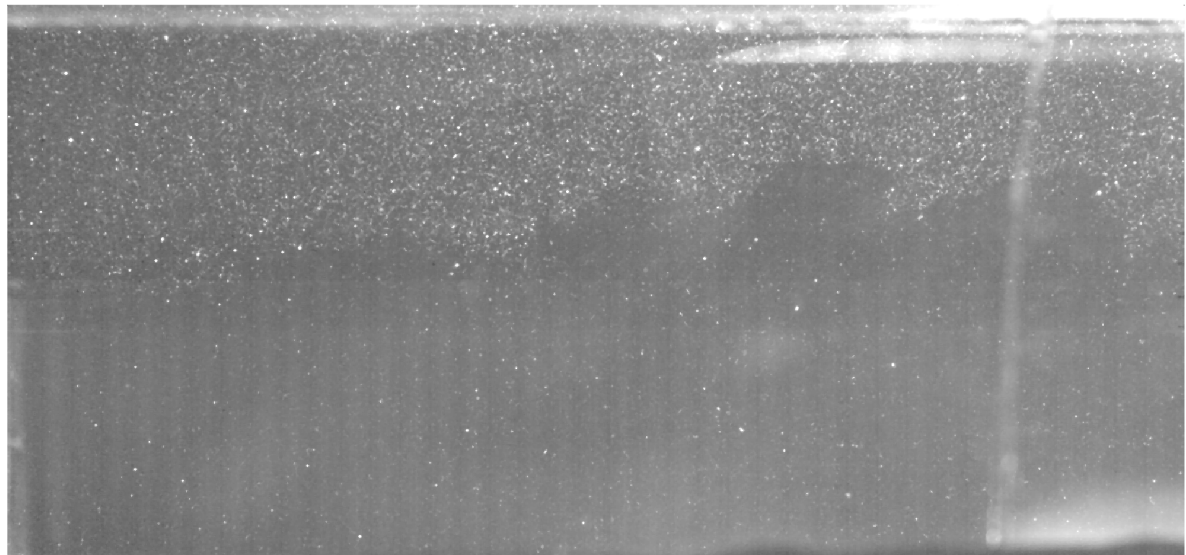


Figure 27: Median filtered image A

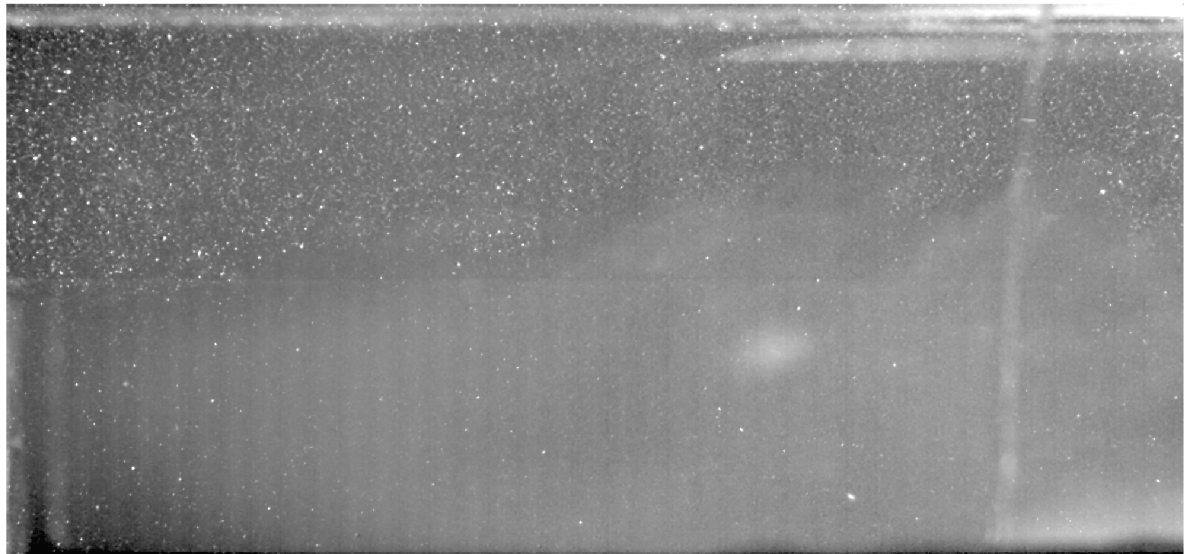


Figure 28: Median filtered image B

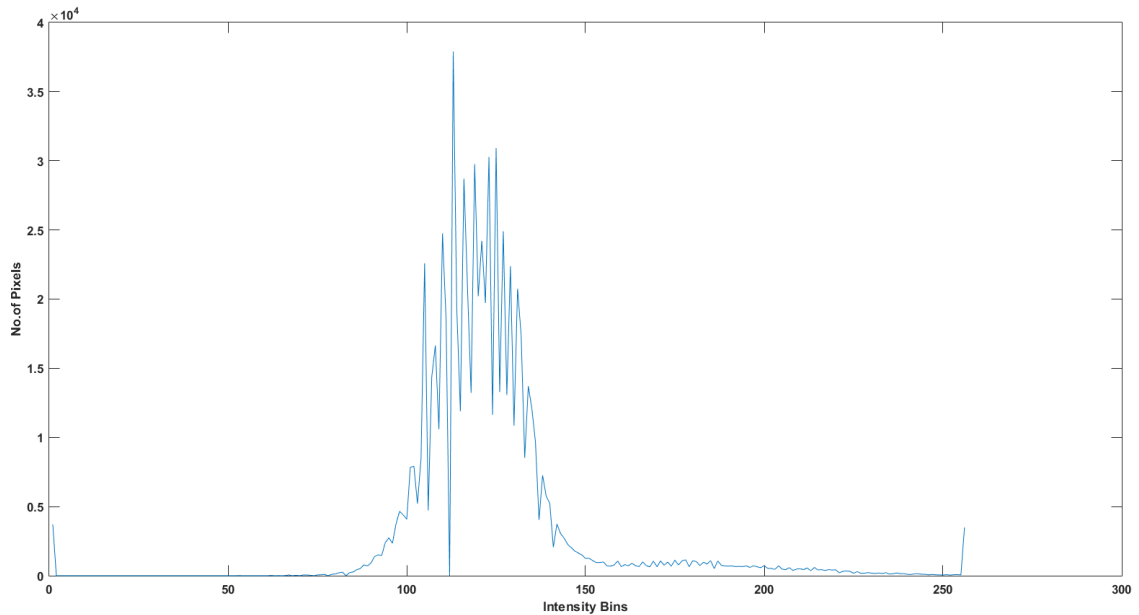


Figure 29: Intensity Histogram of A after median filtering

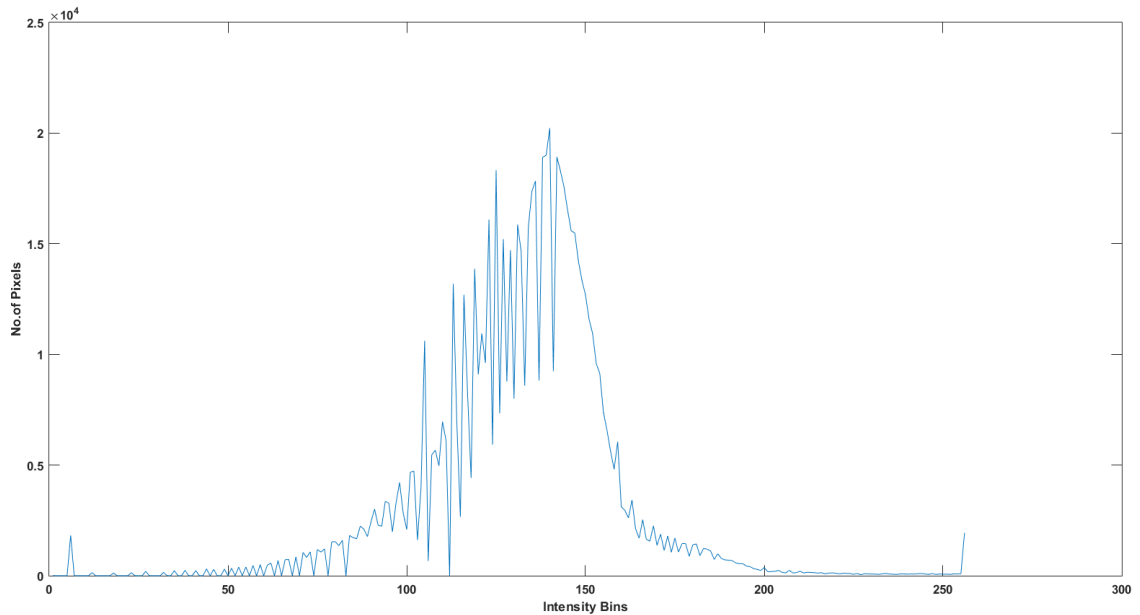


Figure 30: Intensity Histogram of B after median filtering

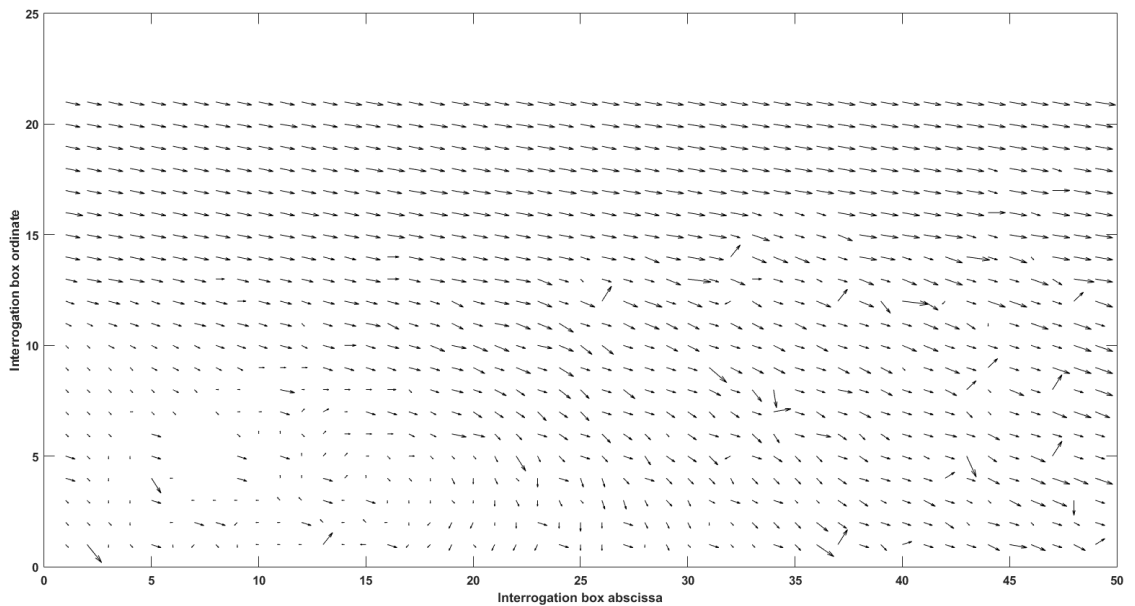


Figure 31: Vector field after Median filtering

### Median filter

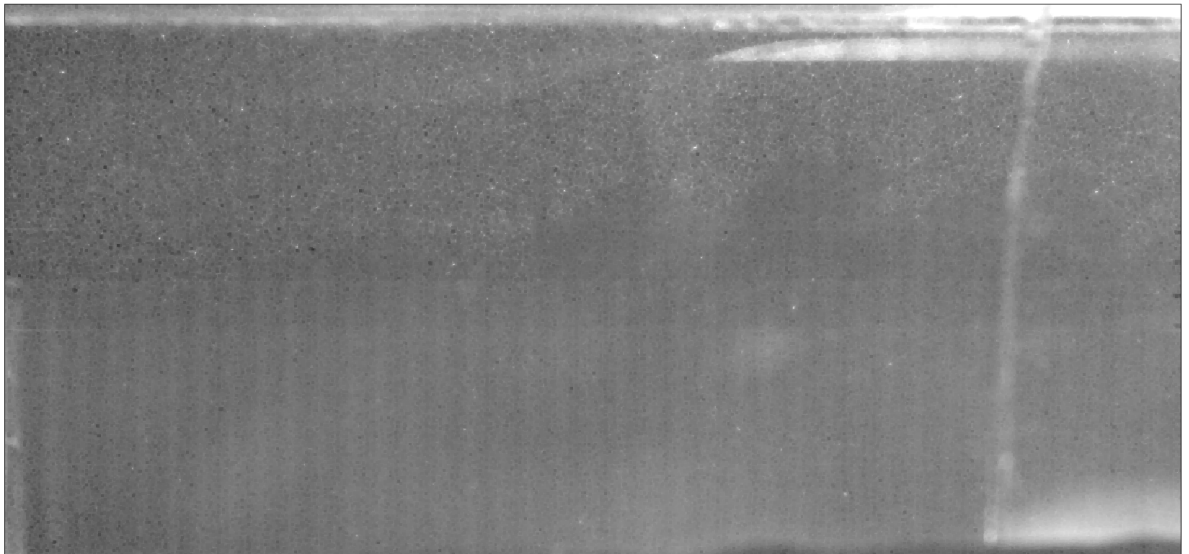


Figure 32: Minimum filtered image A

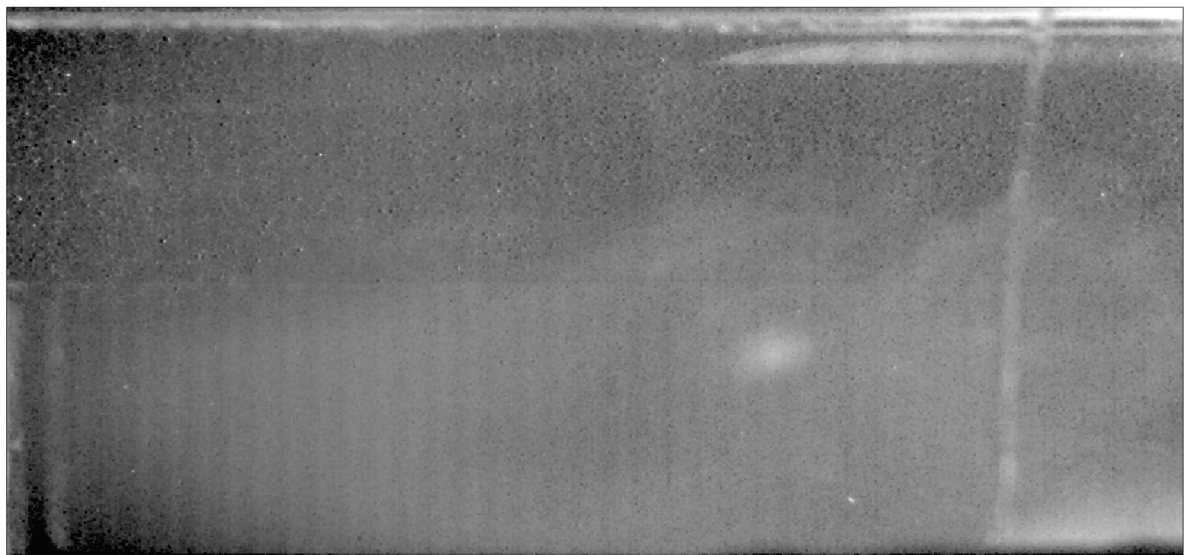


Figure 33: Minimum filtered image B

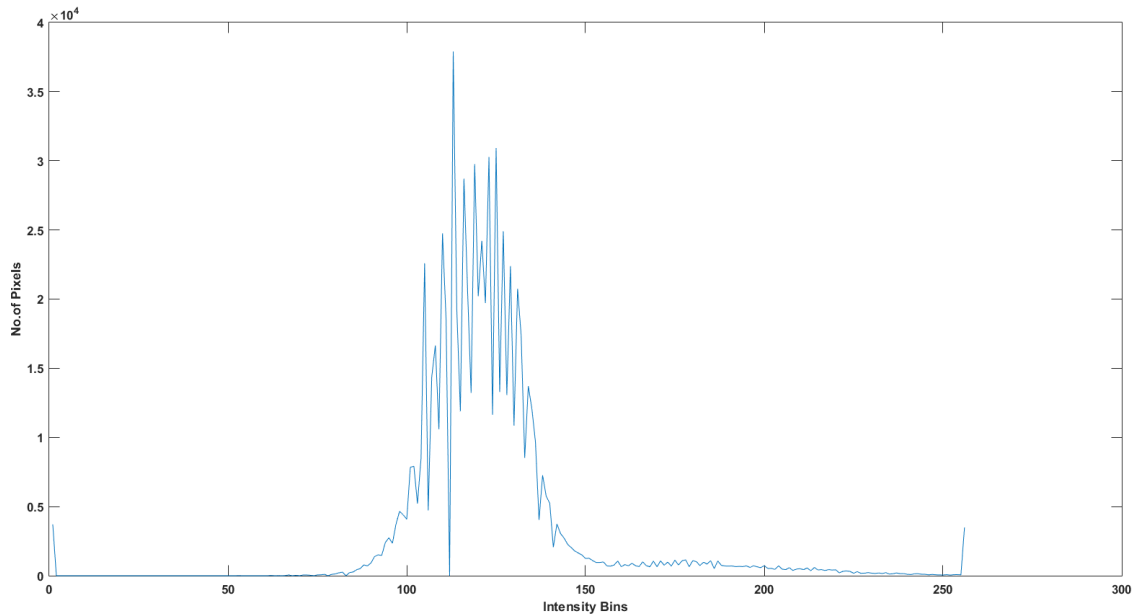


Figure 34: Intensity Histogram of A after minimum filtering

**Minimum filter** ,

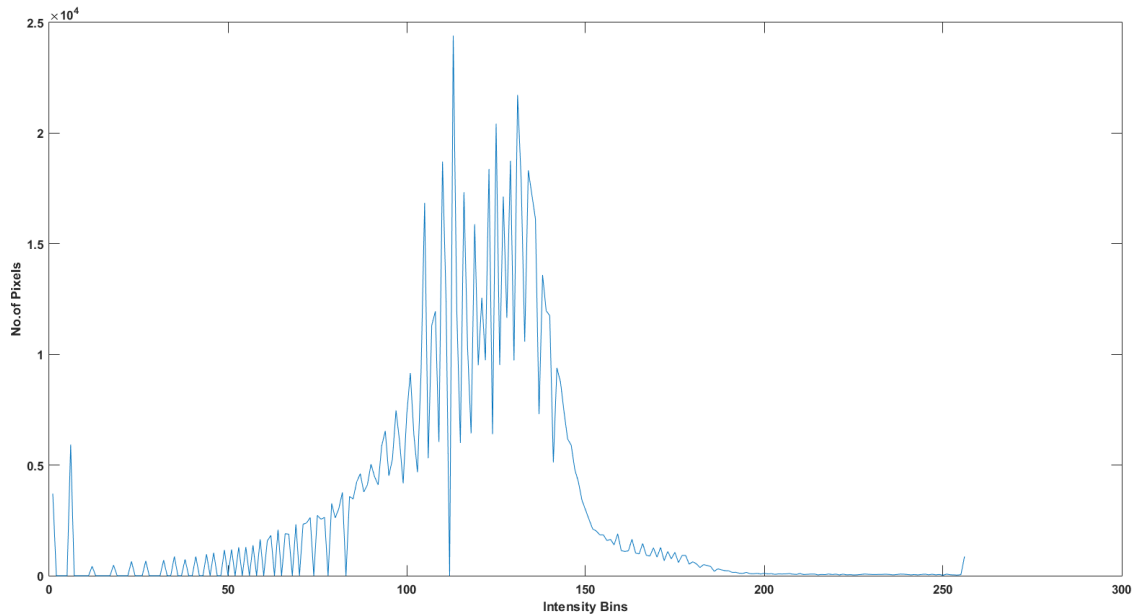


Figure 35: Intensity Histogram of B after minimum filtering

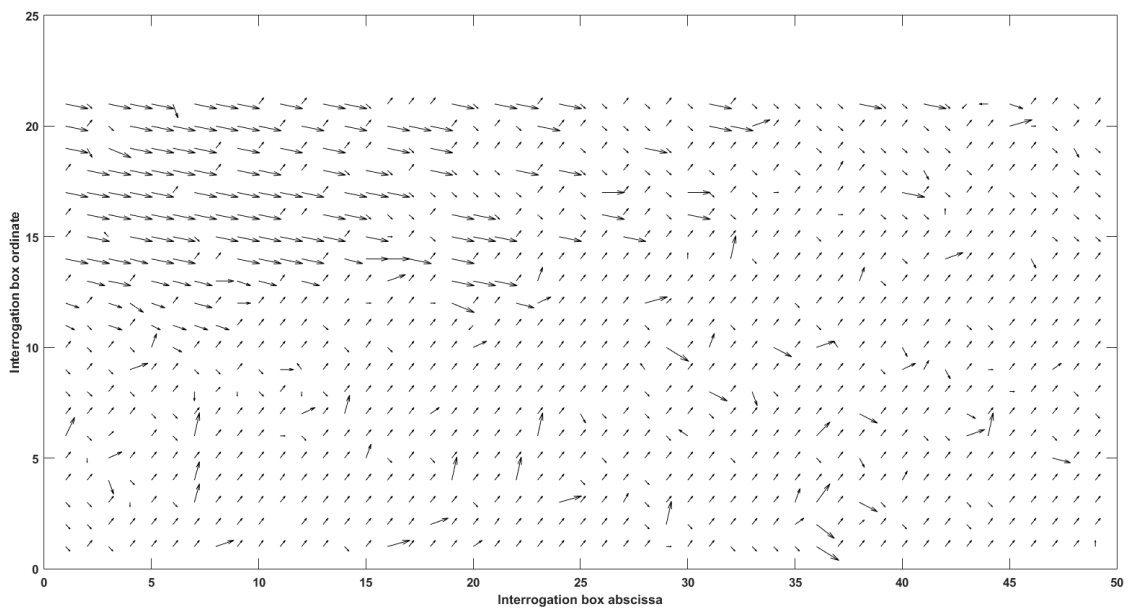


Figure 36: Vector field after Minimum filtering



Figure 37: Maximum filtered image A

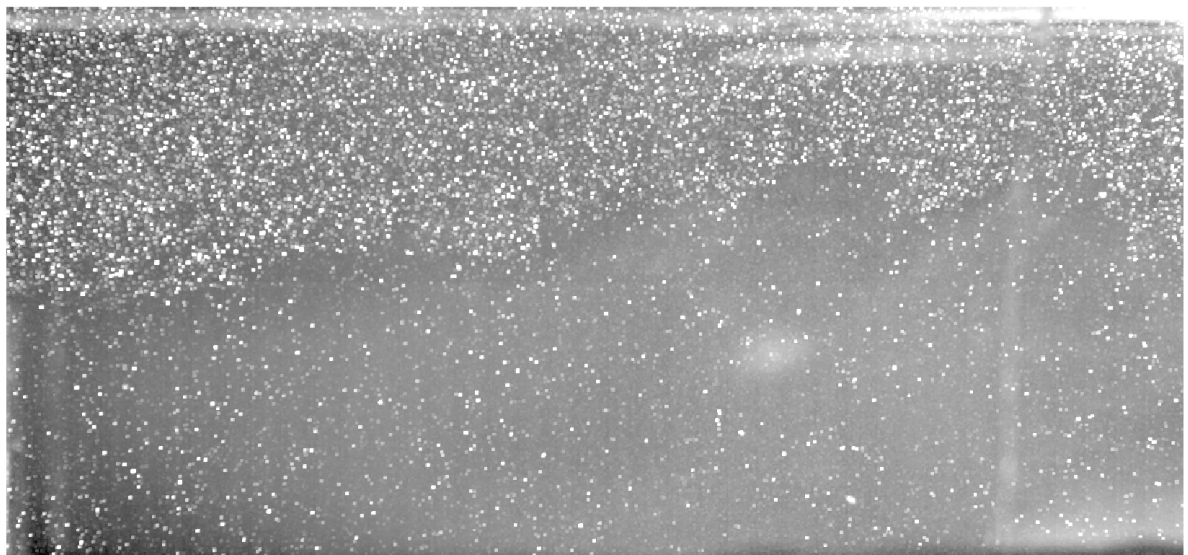


Figure 38: Maximum filtered image B

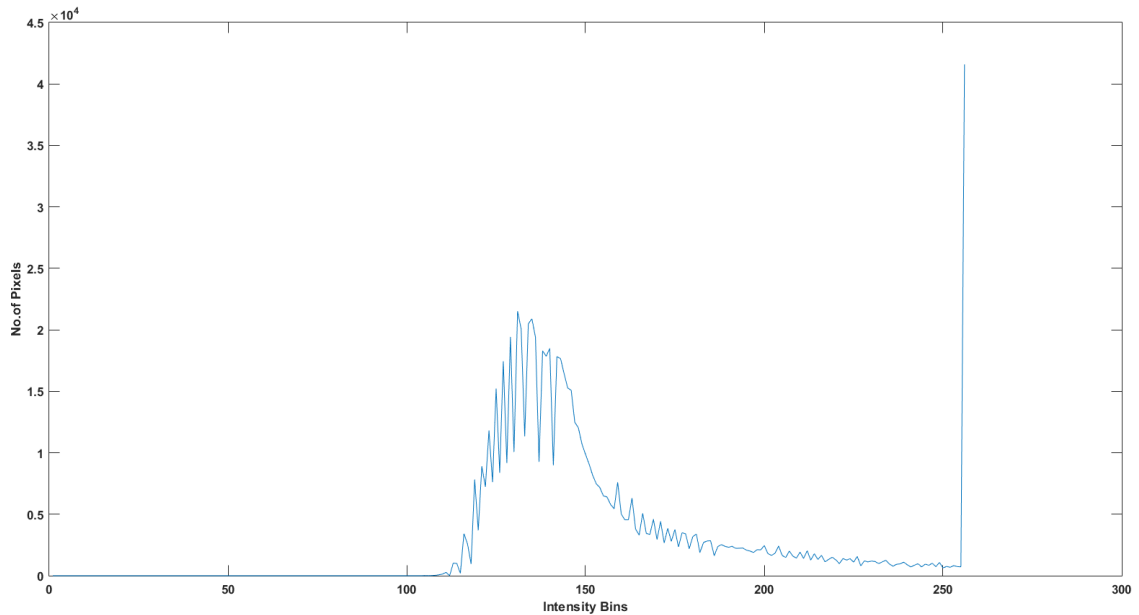


Figure 39: Intensity Histogram of A after maximum filtering

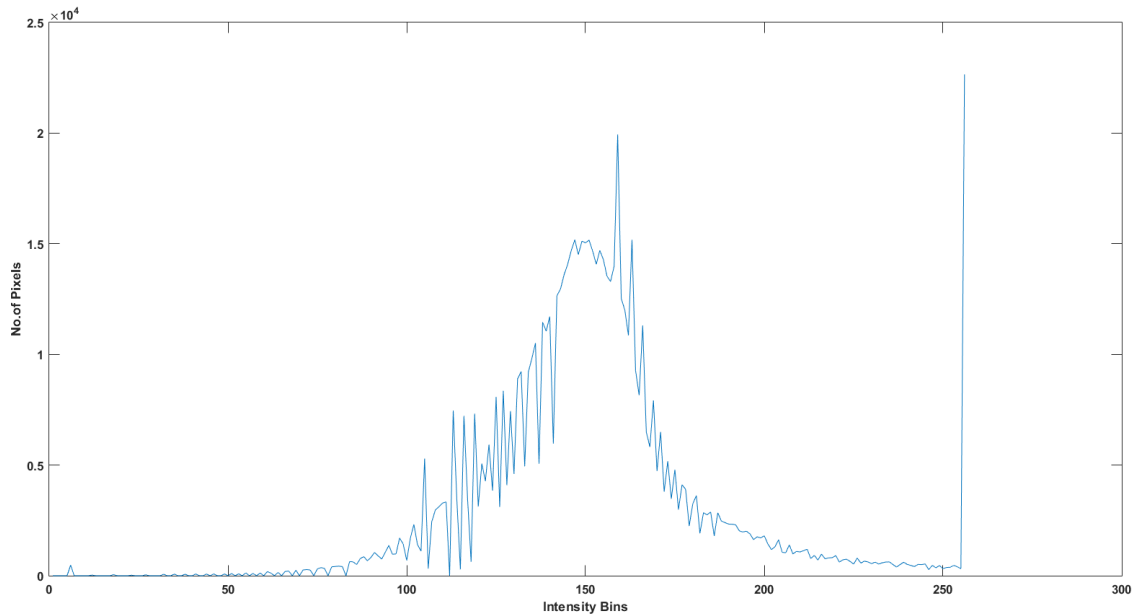


Figure 40: Intensity Histogram of B after maximum filtering

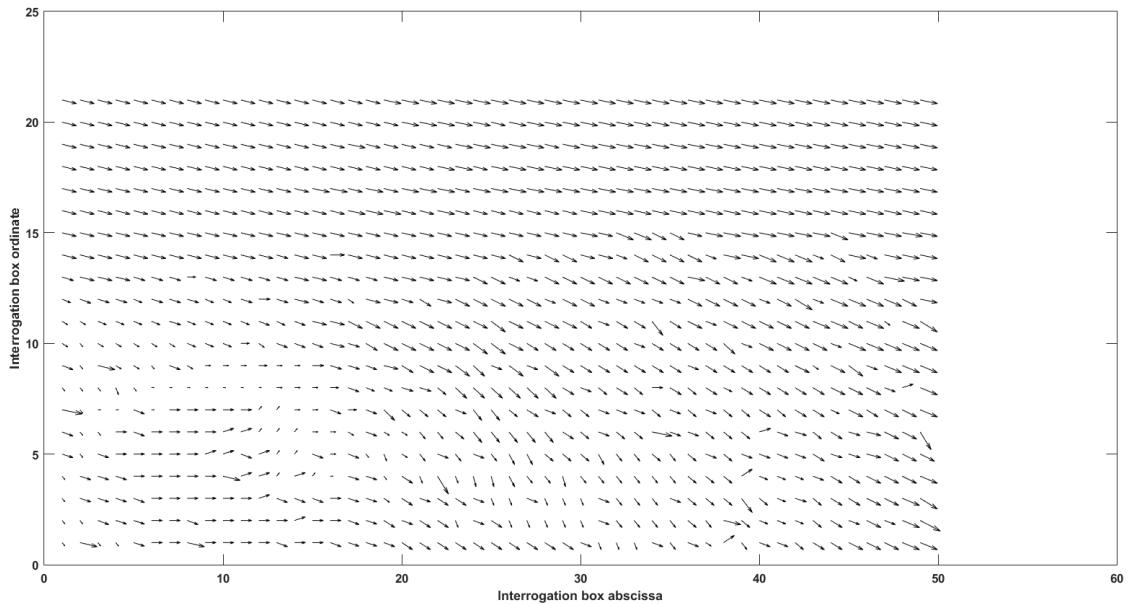


Figure 41: Vector field after Maximum filtering

## Maximum filter

### 4.4.2 Low and High Pass filters

Low pass and High pass filters correspond to eliminating certain range of intensities from the image and performing analysis only on the remaining values of the intensity spectrum, there are various implementations for these filters and sharpening an image is one of them. Nevertheless we implement here brute forced low pass and high pass filters and visualize the results.

**Low pass filter(75%)** We remove the higher 25 % (192-256) values in the spectrum range and visualize.

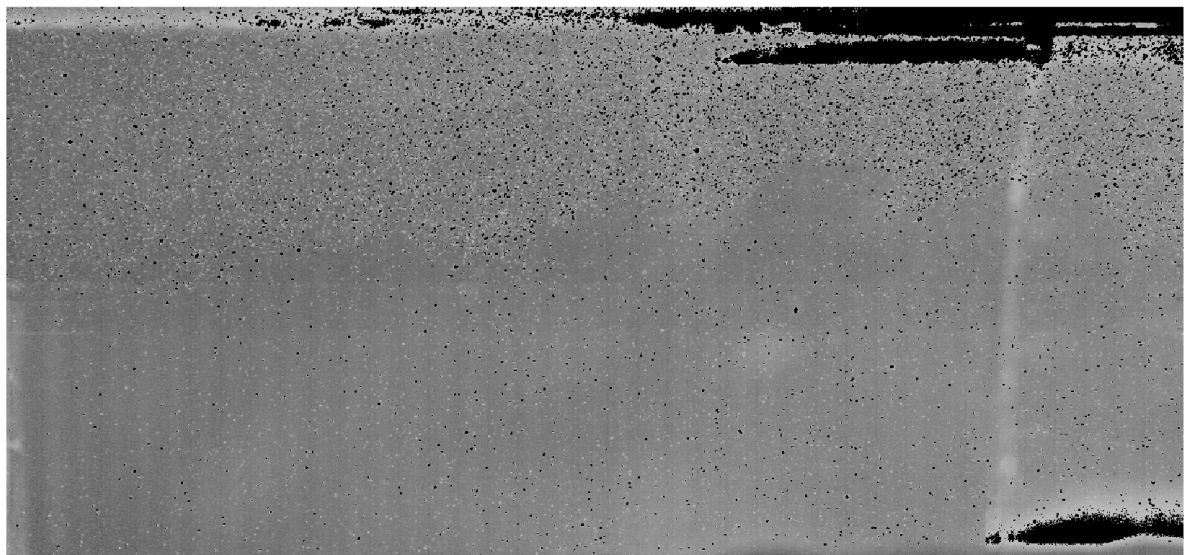


Figure 42: Low pass filtered image A

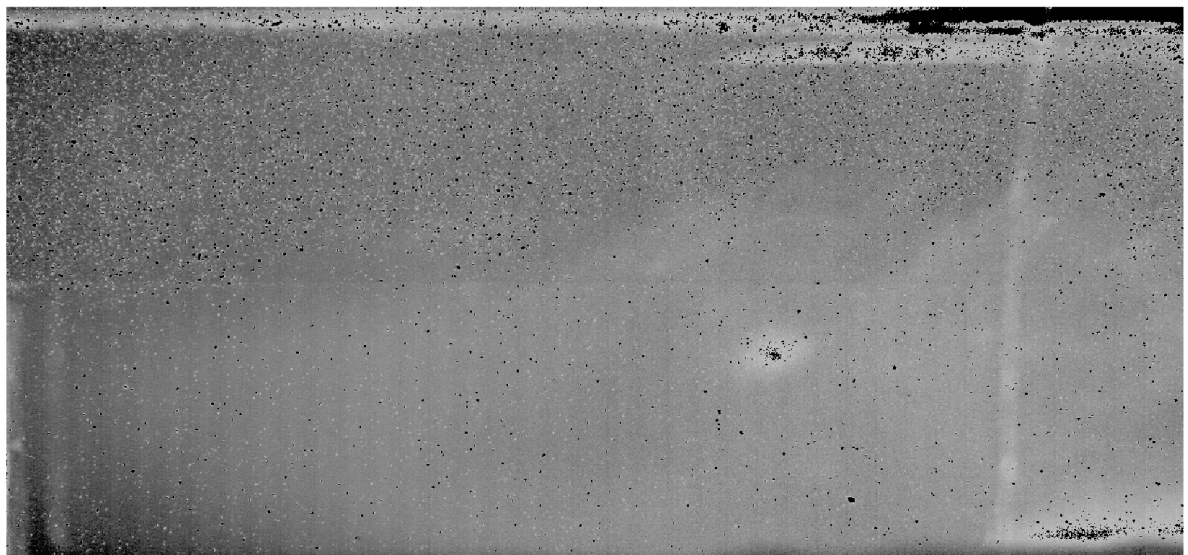


Figure 43: Low passfiltered image B

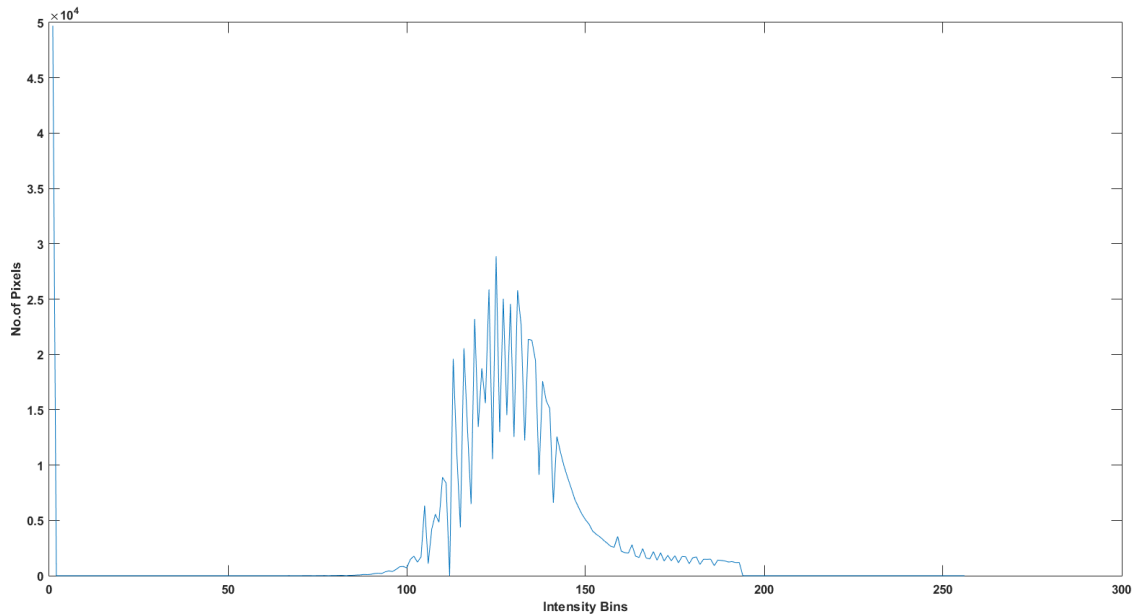


Figure 44: Intensity Histogram of A after low pass filtering

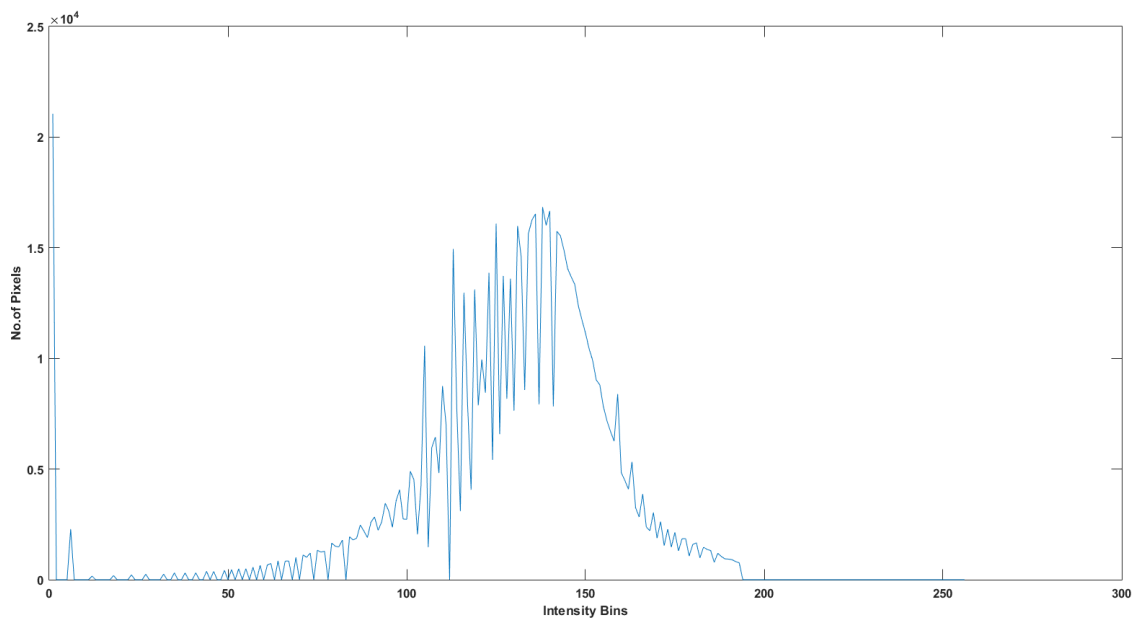


Figure 45: Intensity Histogram of B after low pass filtering

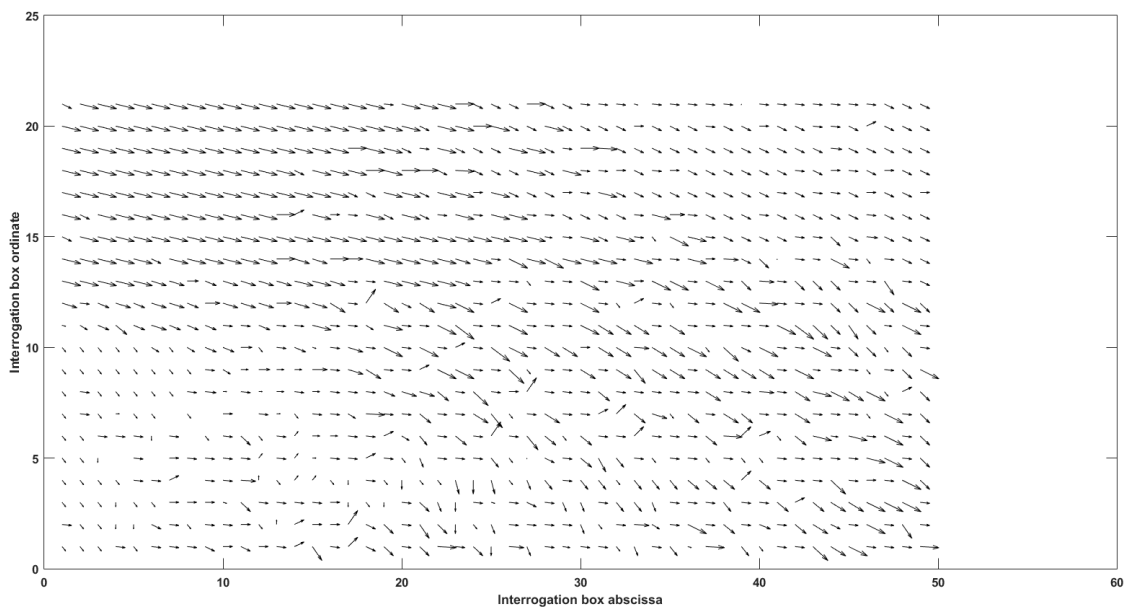


Figure 46: Vector field after Low Pass filtering

**High pass filter(50%)** We remove the lower 50%(0-128) values in the spectrum range and visualize.

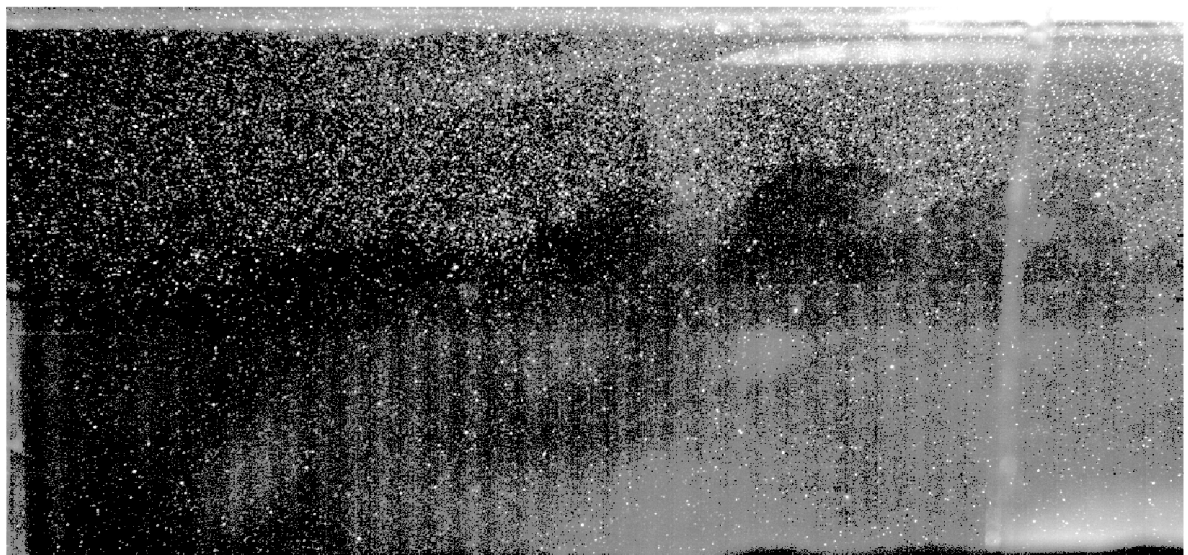


Figure 47: High pass filtered image A

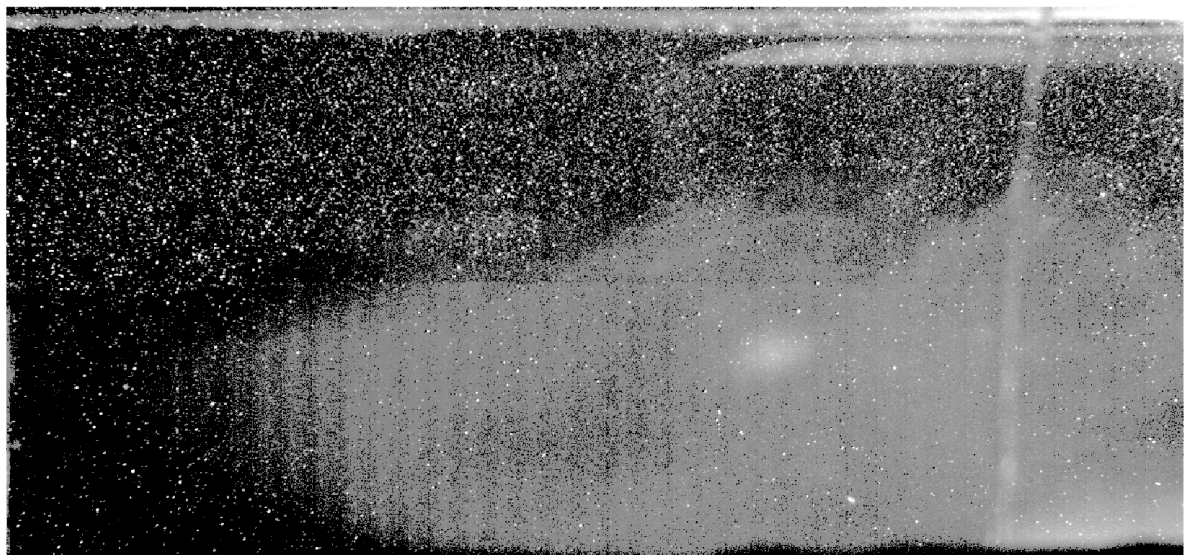


Figure 48: Low passfiltered image B

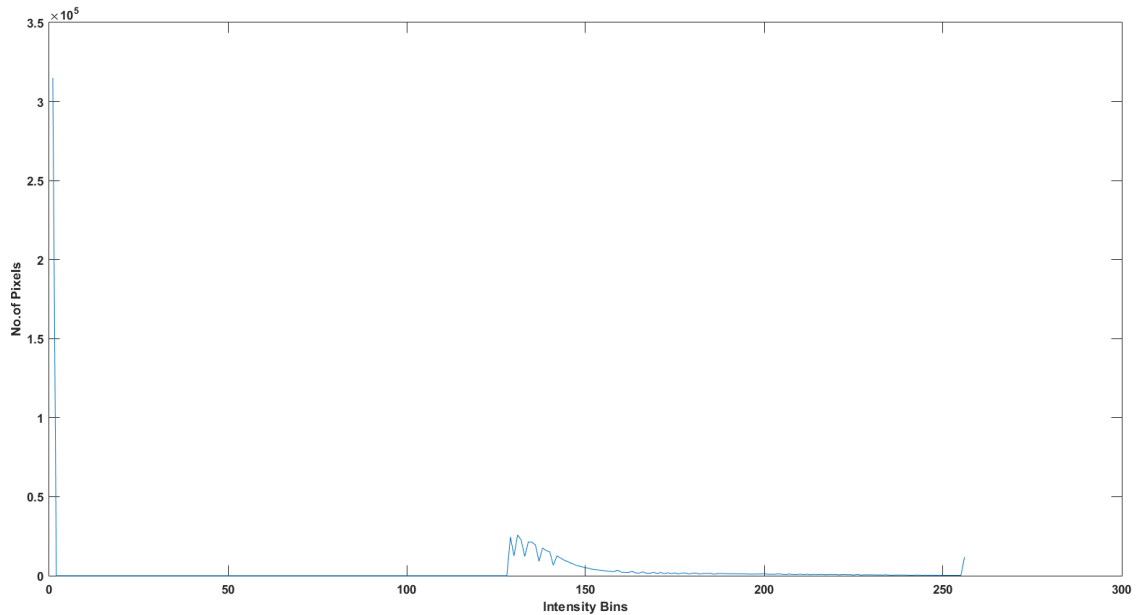


Figure 49: Intensity Histogram of A after high pass filtering

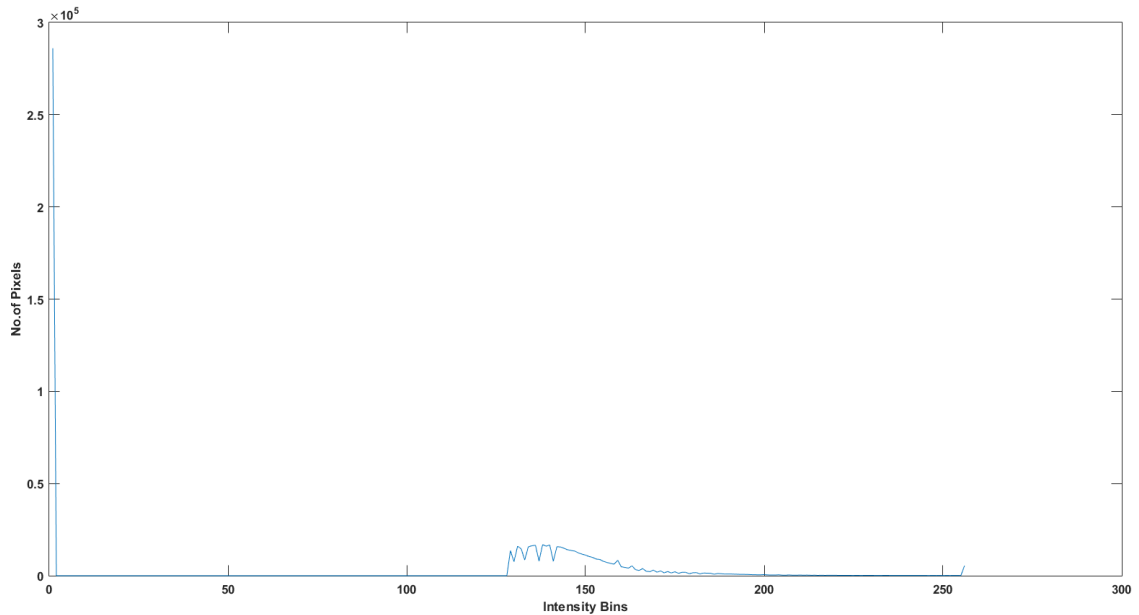


Figure 50: Intensity Histogram of B after high pass filtering

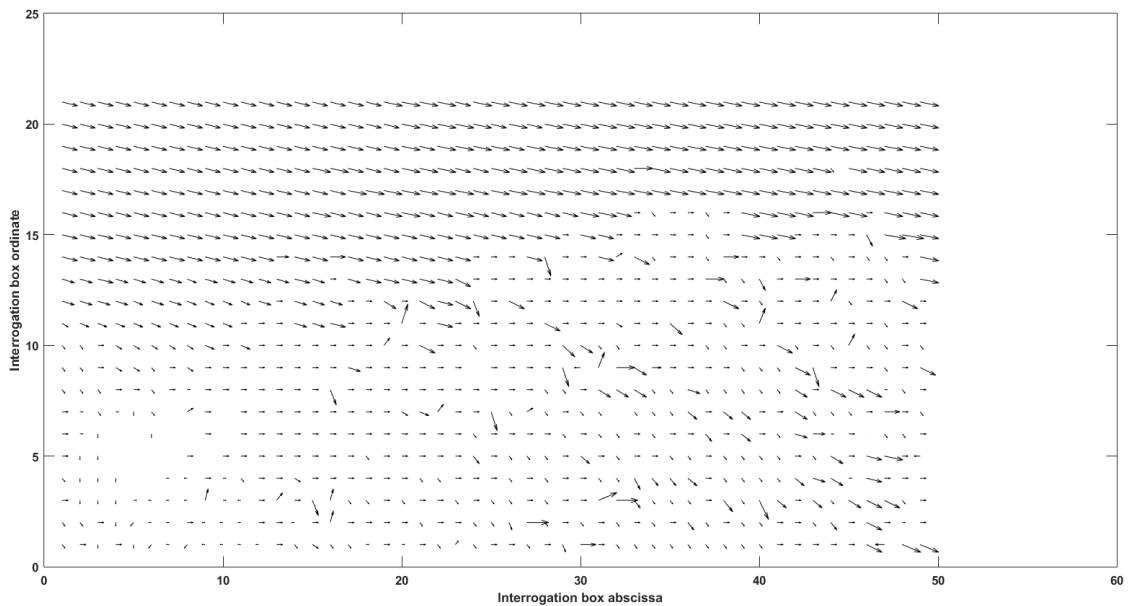


Figure 51: Vector field after High Pass filtering

Filtering	Outlier %	Histogram SD of image A	Histogram SD of image B
Median	0.097	6.41E+03	4.95E+03
Minimum	13.02	6.55E+03	4.90E+03
Maximum	0	5.38E+03	4.49E+03
Low pass	0	6.51E+03	4.67E+03
High pass	0	2.00E+04	1.82E+04

## 5 Results

We shall tabulate our observation fo each of the techniques used,

Technique	Observation	Inference

Technique	Observation	Inference
Histogram Equalization	The image looks a bit more contrasty and the histogram tell us the same. The non uniformities in the intensities increase. A very small percentage of outliers still persist.	We will not be able to use these as we still have higher than raw non uniformities in the intensity histogram.
Sharpening	The image looks a lot more contrasty and the histogram shows a bell curve with additional peak at the higher end. The non uniformities in the intensities decrease. Outliers do not exist.	This has very high chance of being one of the best the candidate solution if not the best as all our problems seem to be solved here.
Median Filter	The image looks blurred and relatively higher intensity pixels seem to increase in the area. The non uniformities in the intensity increase. A very small percentage of outliers still persist.	We will not be able to use this image as the peak detection in the cross correlation might be skewed because of the spread on intensities.
Minimum Filter	The image no more has very high intensity pixels i.e. all our particles of interest vanish. Outliers are very high and the non uniformities in the intensity increase.	We are unable to find any solution resolving to our particles of interest missing.
Maximum Filter	The image has high intensities spreading all around, making the image overall brighter and allowing us to spot out particles more easily(though not accurately). There are no outliers and all non uniformities in the intensities decrease.	Though we will be able to find out locations where our peak exists they may not be accurate as all surrounding points also have the same very high intensity. Nevertheless this can be used in combination with advanced techniques like gaussian peak detection to get a very accurate solution in the cross correlation.

Technique	Observation	Inference
Low Pass Filter	The image no more has very high intensity pixels i.e. all our particles of interest vanish. There are no outliers and non uniformities in the intensity increase.	We are unable to find any solution resolving to our particles of interest missing.
High Pass Filter	The image has accurate very high intensity pixels shown in the image. The non uniformities in the intensities drastically reduce though the contrast doesn't improve as the intensity range also decreases. No outliers exist.	This seems like the best solution we have come across until now but the velocity field doesn't look as accurate as the forward motion of the very high intensitty particles is dominating the vortex effects below the step. We can still use this to a good measure owing to the reduction in intensity non-uniformities.

## 6 Conclusion

We hence implemented image processing techniques for a flow undergoing combustion instabilities whose particles of interest are chemiluminiscent. We see how some of the widely used techniques fail or greatly improve our analysis and velocity fields. We have also seen that some might emphasize improvement in certain flow properties while still improving the overall analysis quality like high pass filters.

## 7 Analysis Code

```

clear all;
clc;
close all;

A = imread('im1.tif');%mat2gray(imread('im1.tif'));%image 1
B = imread('im2.tif');%mat2gray(imread('im2.tif'));%image 2
% F = 128;
% A(A<F)=0;
% B(B<F)=0;
% A = ordfilt2(A,9,ones(3,3));
% B = ordfilt2(B,9,ones(3,3));

```

```

% A = imsharpen(A);
% B = imsharpen(B);
% A= histeq(A);
% B = histeq(B);

[Xmax,Ymax] = size(A);

%window despcrition
winsize = 24;
wins = [winsize,winsize];%16,24,32
winx = wins(1);
winy = wins(2);
% interrogation grid
gridx = 2*winx:winx:Xmax-2*winx;
gridy = 2*winy:winy:Ymax-2*winy;
%displacement matrices initialize
countx = length(gridx);
county = length(gridy);
dx(countx, county) = 0;
dy(countx, county) = 0;

%Cross correlation over all interrogation boxes
for i = 1:countx
    for j = 1:county
        x0 = gridx(i);
        y0 = gridy(j);
        win0 = A(x0:x0+winx-1,y0:y0+winy-1);
        win = B(x0-(winx):x0+(2*winx)-1,y0-(winy):y0+(2*winy)-1);
        %peak finding
        try
            c = normxcorr2(win0,win);
            [peakx, peaky] = find(c==max(c(:)));
            peakx = peakx -winx+1;
            peaky = peaky -winy+1;
            peakx = peakx(1);
            peaky = peaky(1);
            dx(countx-i+1,j)=peakx-winx;
        end
    end
end

```

```

dy(countx-i+1,j)=peaky-winy;
catch
dx(countx-i+1,j)=0;
dy(countx-i+1,j)=0;
end
end
end

%quiver
I = quiver(dy,-dx);
I.Color = 'black';
histA = imhist(A);
histB = imhist(B);
stdhA = std(histA);
stdhB = std(histB);
Ix =I.UData;
Iy =I.VData;
avgIx = mean(mean(Ix));
stdIx = std(std(Ix));
avgIy = mean(mean(Iy));
stdIy = std(std(Iy));

%outlier removal
Ix(Ix>=avgIx+stdIx | Ix<=avgIx-stdIx ) = avgIx;
Iy(Iy>=avgIy+stdIy | Iy<=avgIy-stdIy ) = avgIy;
I.UData = Ix;
I.VData = Iy;
I = quiver(Ix,Iy);
I.Color = 'black';

%outlier % calculation and interpolation of outliers with averaged values
logicalIx = bsxfun(@gt, Ix, avgIx+0.95*stdIx)| bsxfun(@lt, Ix, avgIx- 0.95*stdIx);
logicalIy = bsxfun(@gt, Iy, avgIy+0.95*stdIy)| bsxfun(@lt, Iy, avgIy- 0.95*stdIy);
logicalI = logicalIx|logicalIy;
logiclenI = length(logicalI(logicalI==1));
outlier_percent = 100*logiclenI/(countx*county);

```

```
%command window inputs for filtered/enhanced images and their respective %intensity histograms  
%imshow(A)  
%imshow(B)  
%ax = gca,plot(histA),ax.FontWeight = 'bold',ax.XLabel.String = 'Intensity Bins',ax.YLabel.String = 'No  
%ax = gca,plot(histB),ax.FontWeight = 'bold',ax.XLabel.String = 'Intensity Bins',ax.YLabel.String = 'No  
  
%Vector field window configuration  
ax = gca;  
ax.XLabel.String = 'Interrogation box abscissa';  
ax.YLabel.String = 'Interrogation box ordinate';  
ax.FontWeight = 'bold';
```